GRID IMPACT OF WIND ENERGY ON ISOLATED AND REMOTE POWER SYSTEM

SHEIKH MOMINUL ISLAM

Grid Impact of Wind Energy on Isolated and Remote Power System

By

© Sheikh Mominul Islam

A thesis submitted to the School of Graduate Studies in partial fulfillment of the
requirements for the degree of Master of Engineering

Faculty of Engineering and Applied Science
Memorial University of Newfoundland

July 2009

St. John's   Newfoundland   Canada

To my Parents and Siblings

Abstract

In this thesis, the impact of wind energy on isolated wind-diesel hybrid grid system and on remote grid connected wind farm were studied. In the case of the wind-diesel system a detailed mathematical model of Cartwright grid system is presented. The impact of a grid connected wind farm near St. Anthony, Newfoundland was also studied. Initially a pre-feasibility study was conducted to size the wind farm depending on wind data and local load data. In both cases voltage fluctuation and frequency variation in the grid power system due to the addition of wind energy were studied. Optimization software tool HOMER was used for pre-feasibility study for wind farm in St. Anthony. Detailed dynamic models of all system components and system parameters are provided in the thesis. MATLAB-SIMULINK was used for both cases for the dynamic modeling and system analysis. Finally, results are presented in both cases and future studies are proposed.

Acknowledgement

Table of Contents

List of Tables

List of Figures

List of Symbols

Symbols

m	Air mass
v	Air velocity
E	Kinetic energy
$\dot{m}$	Mass flow rate
ρ	Air density
A	Rotor swept area
C_P	Rotor performance co-efficient
λ	Tip speed ratio
V_u	Peripheral velocity
V_l	Wind velocity
α	Blade pitch angle
T_T	Turbine aerodynamic torque
T_g	Generator torque
T_L	Torque into the gear box
T_H	Torque out of the gear box
J_T	Turbine moment of inertia
J_g	Generator moment of inertia
J_{grt}	Gear box Moment of inertia in wind turbine side
J_{grg}	Gear box Moment of inertia in generator side

J	Moment of inertia
D_T	Turbine damping co-efficient
D_{grt}	Gear box damping co-efficient in wind turbine side
D_{grg}	Gear box damping co-efficient in generator side
D_g	Generator damping co-efficient
K_{grt}	Gear box stiffness in wind turbine side
K_{grg}	Gear box stiffness in generator side
K_T	Stiffness of wind turbine
K_g	Stiffness of generator
g_r	Gear box ratio
J_{equ}	Equivalent moment of inertia
d	Direct axis
q	Quadrature axis
l	Leakage variable
s	Stator variable
r	Rotor variable
m	Magnetizing quantity
R	Resistance variable
I	Current variable
V	Voltage variable
ω	Stator angular electrical frequency
ω_b	Rotor angular electrical base frequency
ω_r	Rotor angular electrical speed

X	Reactance variable
X_m	Mutual inductance
L	Inductance variable
φ	Flux variable
μ	Permeance variable
λ	Flux linkage variable
p	d/dt
P	No of generator pole
N	Winding number
e	Induced emf
Z	Winding impedance
Φ_m	Mutual flux
P_l	Leakage path permeance
P_m	Mutual path permeance
Δx	Elemental length of transmission line
G	Conductance
C	Capacitance
Y	Admittance
γ	Propagation constant
Z_c	Characteristic impedance
f	Forward wave variable
b	Backward wave variable
k	Damping winding variable

f	Field variable
V_d	DC voltage variable
I_d	DC current variable
α	Firing angle
Δi_d	Change in dc current
u	Commutation angle

Chapter 1

Introduction

1.1 Background

For human development to carry on, it is necessary to find the sources of renewable or virtually unlimited energy. It is difficult to imagine this, but even if we find several hundred or even thousand years of coal and natural gas supplies, what the human being will do after thousand of years. Even the most apparently "persistent" sources like fusion involve the generation of large amounts of waste heat enough to place damaging stress on even a robust ecosystem like Earth's, at least for the organisms that depend upon stability of the system. Wind is one of the cleanest and inexhaustible energy among all renewable energy sources [1]. The first windmills on record were built by the Persians in approximately 900AD. The history of wind power shows a general evolution from the use of simple, light devices driven by aerodynamic drag forces; to heavy, material-intensive drag devices; to the increased use of light, material-efficient aerodynamic lift

devices in the modern era. Wind farms were developed first in the United States in the late 1970s and then in Europe in the late 1980s in Denmark.

During the last two decades it is observed that the increase in electricity demand and environmental concerns resulted in a fast growth of power production from renewable energy sources. Among all renewable sources wind energy is one of the most cost effective forms to generate electrical power. Statistical data shows that worldwide capacity reached 121,188 MW, out of which 27,261 MW were added in 2008 [1]. Wind energy continued its growth in 2008 at a rate of 29 %. All wind turbines installed by the end of 2008 worldwide are generating 260TWh per annum, equaling more than 1.5 % of the global electricity consumption [1]. In Canada, government initiatives to advance the expansion of wind energy were implemented moderately later than in many other countries around the world. However, since 2001, Canadian wind energy has grown from faintness to one of the world's largest and fastest growing markets, driven largely by national production incentives and provincial renewable energy targets. These targets have obligated the largely provincial owned utilities and related entities in Canada to procure large blocks of renewable energy, especially wind energy, through power calls that have ranged in scale from 100 kW to 1,500 MW. GWEC (Global Wind Energy Council) reports that Canadian provincial governments are currently seeking to put in place a minimum aggregate of 10,000 MW installed wind power capacity by 2015 which is shown in figure 1.1[2].
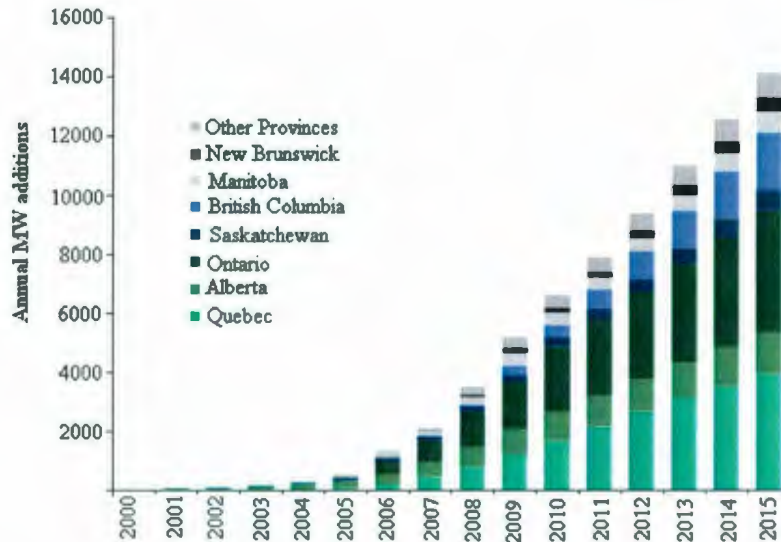
Figure 1.1: Expected annual MW additions in different provinces of Canada

Presently, wind farms in Canada have a capacity of 2,775 MW. That is considered enough to power over 840,000 homes or equivalent to about 1 % of Canada's total electricity demand. Canada's wind resource is well distributed in rural areas throughout the country with 87 wind farms in operation, and more now under construction [2]. There is only one 27MW wind farm in Newfoundland and another 27MW wind farm is under construction.

1.2 Wind farm infrastructure

Wind turbines can be divided into two main categories: fixed speed and variable speed. A fixed-speed wind turbine generally uses a Squirrel Cage Induction Generator (SCIG) to convert the mechanical energy from the wind turbine into electrical energy. The fixed speed SCIG consumes reactive power and cannot contribute to voltage control. Variable-speed wind turbine can offer increased efficiency in capturing the energy from wind over a wider range of wind speeds, along with better power quality and the ability

to regulate the power factor, by either consuming or producing reactive power. Wind turbines operate as part of larger power producing and consuming systems such as large electrical networks, isolated diesel-powered systems or as a stand alone power for a specific load. In addition to the individual wind turbines and their switchgear, wind farms have their own electric distribution system, roads, data collection and support personal.

1.2.1 Electric distribution system and roads

The electrical distribution system in wind farms typically operates at higher voltages than the turbine generator voltage in order to decrease resistive losses on the way to the substation at the grid connection. The voltage levels of the wind farm distribution system depend on the distances between turbines and transformer and the cable costs. Modern wind turbines come with an installed transformer in the tower base but groups of lower voltage wind turbines in close proximity could share one transformer for cost reduction. Access roads between wind turbines and connecting and maintenance roads to highway may represent a significant cost especially in environmentally sensitive areas with rough terrain.

1.2.2 Data collecting system

Modern wind farms include systems for controlling individual wind turbines and displaying and reporting information on the wind farm. Information about the whole wind farm sets of turbines or individual turbine can be displayed by supervisory control and data acquisition system (SCADA). The information typically includes turbine operating states, power level, total energy production, wind speed and direction,

maintenance etc. SCADA system connected to modern turbines may also display oil temperatures, rotor speed, pitch angle etc.

1.3 Wind farm technical issue

The installation of wind farms requires a significant amount of planning, coordination and design work. Mistakes can be very costly. Before wind farms can be installed and connected to an electrical system, the exact locations for the future turbines need to be determined. Once locations for the turbines are chosen, the installation and integration of wind farms into large grids requires obtaining permits, preparing sites, erecting turbines and getting them operational. Once installed, significant interactions can occur between individual wind turbines and between wind turbines and the electrical system to which they are connected. Inadequate consideration of characteristic of the grid at the point of connection can result in unwanted disturbances in the local power system and also can affect other users of the grid.

Interconnection issues include problems with steady state voltage variation, frequency variation, flicker and islanding. Depending on the country, voltages at distribution points are allowed to fluctuate within + 10% of the nominal value [3]. The purpose of this thesis is to study the impact of voltage and frequency variation with the addition of wind turbine to the isolated diesel driven electrical system of Cartwright and adding a wind farm to the electrical grid system in the area of St. Anthony in the province of Newfoundland and Labrador. Both sites are located in high average wind region in Canada. Load data in both cases were collected from Newfoundland Hydro and wind data from the website of weather office.

1.4 Outline of thesis

After providing the general idea about wind turbine and wind farm impact on electrical system in this chapter, the main topics of the thesis are outlined. The reviews of the literature are discussed in the second chapter. In this chapter the scope of the research for previous studies with regards to impact of wind diesel and grid connected wind farms are discussed.

In chapter 3 the mathematical models of different components in the wind diesel hybrid power system are developed. A case study is done in chapter 4 to observe the impact of wind turbine in diesel driven electrical system in Cartwright, Labrador. In chapter 5 a grid connected wind farm in St. Anthony, Newfoundland is studied to determine the voltage and frequency variation. The conclusions and recommendations are listed in the last chapter.

Chapter 2

Literature Review

2.1 Introduction

Wind power production is increasing rapidly and more wind turbines are being
connected to power system. The revolution occurred in wind power industry during the
last century. The interest in wind power industry is increasing due to the increasing fuel
prices, and to reduce pollution. The global wind power industry is expanding rapidly [4,
5]. EU countries plan to expand large scale offshore wind farms, 10000 MW by 2010,
including a predictable offshore wind power capacity of 4000 MW in the UK. The target
for installed wind energy is 5500 MW in Denmark by 2030, out of which 4000 MW will
be offshore. In Canada the government has set up the target to increase the wind power
industry to 10000MW by 2015. With the development of wind turbine technology, large
scale wind farms of hundreds MW level are being developed in many countries. Wind
turbines interact with the electrical power system in many ways and for the installation of
wind turbines in large scale, special studies are necessary to determine the impact over

7

the system power quality and stability. A number of researchers have studied grid integration issues of wind turbine and wind farm during the last decades. In Canada still wind energy is mostly unexplored and there is a huge potential. The following sections discuss the issues of grid integration of wind farm and the impact of wind turbine on a diesel powered electrical system.

2.2 Grid integration of wind farm

If wind farms are installed solely to maximize energy output, they would have major limitations in terms of power control, voltage variation, frequency variation, power factor, transient fault behaviors. These are the main issues that should be considered before the connection of wind farm. Some details of past research are given through out the following section.

Tande JOG. [6] tried to give an overview of grid integration of wind farms with respect to impact on voltage quality and power system stability. A procedure is recommended for assessing the impact of voltage quality in grid. To observe the slow voltage variations, load flow analysis is conducted over ten minutes time period. The result of this analysis shows variations within + 10% specified by the power quality standard EN 50160. To improve the voltage quality constraint, power factor modification is recommended. He found that a modest reduction in power factor from unity to 0.98 (inductive) will reduce the maximum voltage by 1.5% and hence will reduce the voltage variation on customer side. But again he found with this solution, a reduced power factor will increase network losses. The output power from wind farms may vary significantly within a few seconds and depending on the applied wind turbine technology. He found

8

that sufficient and fast control of reactive compensation is required to relax voltage stability limitation related to wind farms, which can be provided through the use of wind turbine active control or by using external compensators such as static var compensators (SVCs).

Tande JOG. and Jørgersen P. [7] suggested a set of parameter should be specified for wind turbines as part of their technical documentation, and the recommended assessment methods described can be applied prior to installing new wind turbines. They predicted the wind turbine's voltage quality to investigate the electrical characteristics of wind turbine. They introduce a set of reference parameters to enable the consistent of the electrical characteristics of different wind turbines. The maximum continuous power from wind turbine is essential for determining the impact on the steady state voltage level. The relation between the maximum continuous power and the reference power depends on the wind turbine design. Reactive power of a wind turbine is also a key element for determining the impact on the steady state voltage level. Operation of wind turbines has an impact on the voltage quality at the connected network. It is found that the impact of wind turbines on the voltage magnitude is most critical if wind turbines and consumers share the same medium voltage feeder. In this paper they found that the wind power gives less voltage deviations the higher the short circuit power. It is also found that the same injection of wind power may give an increment or a decrement in the voltage magnitude depending on the network impedance phase angle. It was suggested that the magnitude of the voltage may be assessed by preparing the load flow analysis.

Tande JOG. and Uhlen K. [8] suggested an assessment of thermal capacity and voltage stability limitations and innovative solutions. These limitations were identified

9

through examples and allowed them a cost effective means to increase the penetration of wind power in weak grids. Load flow analysis was conducted to assess the slow voltage variations. Two load situations were considered to observe the maximum and minimum voltage levels on the minimum voltage lines. The flicker emission from a single wind turbine or from a wind farm due to starts and due to continuous operation can also be assessed. To reduce flicker during at the starting of wind farm can be reduced by allowing less number of wind turbines starting at the same time [8]. They found that flicker emissions due to continuous operation are a limitation for further extension of the wind farm. To overcome this limitation, different types of variable speed wind turbines were selected which give a much lower value for flicker co-efficient. A wind turbine with an induction generator directly connected to the grid without an inverting power electronic converter is not expected to distort waveform. A large wind farm is to be connected at the remote end of wide regional network that also connects to nearby distribution grid with some other local generations. With modest wind power penetration an acceptable level of security is maintained because the local generation is able to supply the main parts of the local load in case of a critical contingency. In normal operating condition high wind penetration will lead to voltage stability problems and thermal over load due to the limited capacity. This constraint can be solved by installing various rating of static var compensators. The regional network can be isolated from the main interconnection at any time when faults occur. In such a case the isolated network may have a large but varying surplus of power due to the wind generation. They propose that application of energy storage and automatic frequency control of the wind turbines may be necessary in order to maintain a continuous supply of power in this situation.

Chen Z. [9] presented the requirements of wind turbine connection with the power system. Wind turbines can be connected to electrical systems in various voltage levels including the load voltage, medium voltage, high voltage as well as to the extra high voltage system. Voltage quality of a wind turbine or wind farms may be assessed in terms of steady state voltage under continuous production of power and voltage fluctuations. The impact of connecting a wind farm on the grid voltage is directly related to the short circuit power level. It is found that the variations of the generated power will result in the variations of voltage at the point of common coupling (PCC). If the short circuit impedance of the network is small then the voltage variations will be small, indicating a strong grid. For large value of short circuit impedance the variation of voltage will be large indicating that the grid is weak. Operation of wind turbines may affect the voltage in the connected network. It is recommended that load flow analysis can be conducted to assess this effect to ensure that the wind turbine installation does not bring the magnitude of the voltage outside the required limits. Fluctuations in the power system voltage may cause perceptible light flicker depending on the frequency and magnitude of the fluctuation. The allowable flicker limits are generally established by individual utilities. Integration of large scale wind power can have greater impact on the connected power system. For future large wind farm active power is regulated linearly with frequency (50Hz electrical system) variations between a certain ranges (47 Hz – 52 Hz). The reactive power should be regulated within a control band at a maximum level of 10% of rated power. In this paper the author has discussed many aspects regarding the potential operation and control methods during the installation of large scale wind power into the power systems.

11

Chuong T.T. [10] addresses the impact of wind power on the voltage at distribution level in his research paper. He presented a method to observe the relationship between the active power and voltage at the load bus to identify the voltage stability limit. A system experiences a state of voltage insecurity when there is a progressive or uncontrollable drop in voltage magnitude after a disturbance, increase in load demand or change in operating condition. The main factor, which causes these unacceptable voltage profiles, is the instability of the distribution system to meet the demand for reactive power. Under normal operating conditions, the bus voltage magnitude (V) increases as reactive power injected at the same bus is increased. Although the voltage instability is a localized problem, its impact on the system can be wide spread as it depends on the relationship between transmitted real power, injected reactive power and receiving end voltage. To overcome the constraints of the bus bar, he proposed that generator and excitation system protection settings and timings will require applying carefully to ensure that wind farms operate within accepted network voltages and machine ratings.

Chen Z. [11] studied the voltage fluctuation and harmonic distortion in a network to which variable speed wind turbines are connected. In his paper he proposed a wind farm comprising a number of wind turbines housing direct drive, variable speed permanent magnet generators and variable speed capability is achieved through the use of an advanced power electronic converter. In his paper he describes that voltage fluctuation and harmonic distortion can be minimized through advanced power electronic converters. In his case study he used a radial distribution system and he kept the slack bus voltage to 1.053 pu and also he considered a constant loading during the analysis with a wind farm total loading capacity of 32%. He performed different power flow analyses with no wind

power connected, with wind power converter operating at P_{min} and unity power factor and with wind power converter operating at P_{max} and unity power factor. He found that unity power factor operation of the wind farm can increase the network voltage level and also he found that the injection of varying power can result in bus voltage fluctuation, although the voltage variation is less than 2% in this case. If the wind power varies over a wider range and the load variation is taken into account, then voltage fluctuations may become unacceptable for loads connected on some buses even though the wind power generation is maintained at unity power factor. He also proposed that the bus voltage fluctuation can be reduced if the wind farm inverters are used to generate reactive power during system low voltage periods and to absorb reactive power during system high voltage periods.

Muyeen S.M. and Shishido S. [12] have shown the necessity of energy capacitor system (ECS) for combining power electronic devices and electric double layer capacitor. Here they showed that ECS can significantly reduce voltage and power fluctuation of grid connected wind farm. To verify the effectiveness of their proposed system they performed two case studies using real wind speed data and 275kW wind turbines. In their first cases they found that the generator output and line power are same. In case-1 they found that with a maximum wind speed variation 6m/s the voltage variation is about 11% without using energy capacitor system. With the addition of energy capacitor system they proposed that the voltage variation can be reduced to almost 2%. It is proposed that ECS can be used for smoothing the fluctuations of output power and terminal voltage of wind farm under randomly fluctuating wind speed condition. They calculated the line power reference using EMA of wind farm output, instead of using constant line power

13

reference. Finally it is proposed in the research work that a capacitor system can be used in power system to reduce the fluctuations that can be caused by wind farm.

Bialasiewicz J.T. and Muljiadi E [13] explore the effects of wind farm power fluctuations on the power network. They follow a conservative approach to explore a wind farm that consists mainly of stall-controlled wind turbines with fixed frequency induction generators and a specified grid with a known short circuit capacity. It is found that the voltage variation at the PCC is a result of real and reactive power output variations of the wind farm. The variation of reactive power is more dominant in causing the voltage fluctuation at the PCC. Their simulations show that the maximum deviation of the PCC voltage above average value occurs when the reactive power absorbed by the wind farm decreases to low values due to low generation. Thus, this maximum voltage deviation can be correlated to the deviation of reactive and real power below average value. The minimum of the voltage value at PCC occurs when the reactive power absorbed by the wind farm increases to high values. Thus this minimum voltage can be correlated to the deviation of the reactive power above average value. This paper investigates the effects of wind turbine aggregation on a large wind farm. This paper also shows that the more groups used to represent a wind farm, the smaller the fluctuation which means that a wind farm with more small turbines creates fewer power/voltage fluctuations on the power grid than a few large turbines.

Feltes and Erlich [14] introduced a new approach for the coordinated control of voltage source converter based HVDC and wind turbines equipped with doubly fed induction generators. A PI controller is used to regulate the frequency in the wind farm grid to limit the value in desired range. When this control is used to limit the maximum

14

slip considering maximum speed, a slip limitation can be performed at the super synchronous operation. But since rotor power in sub synchronous operation mode is small, this approach shows the best behaviour concerning limitation of rotor power. An increase of wind speed above its nominal value accelerates the rotor of the wind turbine. The pitch control is slow and it takes time to reduce the mechanical torque again, so that the generator can break and finally recover its nominal speed. During this process the variable control can be used to limit the generator slip and also the rotor power. With a wind speed ramp from 12 to 20m/s for fixed frequency operation they found that the frequency variation is about 15%. When the frequency control is operated at constant voltage, the grid and rotor side converter active currents are proportional to rotor and stator active power. With the change of wind speed they found that the full range of voltage fluctuation is + 10%

2.3 Wind Diesel System

Wind – diesel technology is at an exciting stage of development. Research on sophisticated wind-diesel systems is still undergoing. In order to determine the feasibility of wind-diesel system, they must be evaluated. Research is being done to predict fuel savings, power quality, voltage fluctuation, frequency variations etc. This section will discuss the current research works.

Hunter R. and Elliot G. [15] discuss that slow voltage variation can be defined as changes in the RMS value of the voltage occurring in a time span of minutes or more. The voltage variation at the customer's terminal under any condition must not differ from the nominal voltage by more than + 10%. Normally, the frequency of large power

15

systems is very stable (<1% variation). Electrical components and appliances should normally be designed to withstand a frequency variation of at least +3%. So they suggest wide frequency range operation for small diesel grids and wind-diesel systems.

Tsitsovits and Freris [16] developed a computer simulation program to investigate the feasibility of 100% wind penetration in wind diesel power system in isolated network. They simulated the system and developed a computer policy to minimize the voltage and frequency variation due to wind turbulence and load fluctuation. They considered three distinct mode of operation for system steady state operation. One of which is the load supplied by diesel power only, the next one is the load is supplied by wind turbine only and the last one is the load is supplied by wind-diesel hybrid source. During the simulation it was expected that the voltage variation should be within + 10%, the frequency variation should be within + 4% etc. In parallel mode operation the voltage fluctuation was found to be less than 3%. In case of stand alone wind generator mode the frequency variation in uncontrolled system was found almost + 1.5Hz. The range of frequency variation in controlled system is within 50-50.3 Hz. The simulation results in their research are the eigen value analyses of the proposed system indicating that stable operation and acceptable energy quality are achievable with 100% wind penetration except turbulent windy condition.

Jindal A.K., Gole A.M. and Muthumuni D. [17] designed controllers to ensure operation of the wind and diesel units in a cooperative manner to reduce the fossil-fuel consumption of the diesel generator. Wind turbines produce a level of power dependent on the wind passing the rotor at any given instant. As wind is variable in nature, the wind turbine's power output can have fluctuations. The proportion of wind power determines

the level of control required for an electrical system. To evaluate the performance of the wind-diesel hybrid power system, they considered an isolated village with load of 1MW. The load in that village was supplied by diesel generator. The wind turbine is connected with the load through a short over head transmission line of length 2.5 km. From their simulation they found that wind turbine and diesel generator work satisfactorily to meet the power demand with their proposed control system.

Hee S. K. and Jatskevich J. [18] proposed power quality control logic based on Takagi-Sugeno fuzzy model and linear quadratic regulator. They compared this control with the conventional proportional integral controller and shown that it is more effective against disturbances caused by the wind speed and load variations. They considered a system consisting of a horizontal axis 50kW induction generator wind turbine is connected to an ac bus in parallel with a 55KVA turbocharged diesel-synchronous generator. During their simulation they found that with the change of wind speed the change of bus voltage is about 3.4% and the variation of bus frequency is about 2%. Their proposed control scheme provides more effective means to achieve better power quality.

Iglesias I.J., Garcia L., Agudo A., Cruz I. and Arribus L. [19] present a design of an isolated wind diesel hybrid power system with a flywheel energy storage unit. Their main objective was on reducing the fuel consumption by introducing a flywheel which permits the switching off the diesel supply. First the kinetic storage system has been simulated by modelling both the motor and the network side converters. Second the complete wind diesel generator has been simulated with all the elements working together and also the complete control system which maintains both the frequency and

17

voltage of the isolated network. During their simulation they found that with no load the wind turbine is generating a power of 30kW and the flywheel is storing energy. But when suddenly an external load of 50kW is applied then the input wind power remains constant at 30kW and the flywheel will have to supply the additional power to meet the total load demand. It was observed that such a high increment of the load only gives a variation of the frequency up to 49.85Hz.

Fadaeienedjad R., Moschopoulos G. and Moallem M. [20] studied the impact of all electrical, mechanical and aerodynamic aspects of the wind turbine on the power quality of a wind-diesel system. Flicker and voltage variations are induced by load flow changes in the grid and wind speed variation. They found that the flicker emission produced by a Wind Turbine during continuous operation is mainly caused by fluctuations in the output power due to wind speed variations, tower shadow effect, and wind shear effect. The torque and power generated by a wind turbine fluctuate as they are much more variable than that produced by more conventional generators. These fluctuations are due to periodic and stochastic terms. Wind velocity is a stochastic phenomenon continuously changing in direction and speed while wind shear and tower shadow are events that can be categorized as periodic terms. During their simulation they found that how wind speed fluctuations vary the generated power and voltage, where the diesel generator and its controllers, i.e. AVR and governor, try to compensate the variations. From their simulation results they found that the AVR maintains the voltage variations between $0.98pu$ and $1.005pu$, whereas the wind turbine bus voltage varies from $0.92pu$ to $1.04pu$ ($\Delta V1 = 12\%$).

Choi S.S. and Larkin R. [21] studied the behavior of the hybrid diesel-wind turbine power system by assessing the effect of normal variations in the wind mechanical power on system frequency and voltages. It is found that the wind turbines would degrade the quality of the electrical supply by causing unacceptably large voltage and frequency excursions. From their test measurements, they concluded that voltage as well as frequency transients under normal wind turbine operating modes were comparable with those produced by typical load changes on the diesel system alone. From the simulation, the voltage variation at 6.6kV bus was found 5.2%, while a 0.8 Hz frequency change is predicted. These variations are considered excessive under normal planning criteria. In practice, reactive support is likely to be distributed within the wind farm and the loss of some of the induction generators will most probably involve the tripping of some of the capacitive support. The overvoltage problem can therefore be alleviated. The maximum frequency excursion is predicted to be approximately 1.2 Hz.

2.4   Scope of the Thesis

From the above literatures it is found that most of the researchers studied their wind diesel system in labs. Most likely they discussed the control of a wind-diesel system, flicker emission, wind diesel storage system, power quality from a wind farm etc. None in the above listed literature search have done simulation of a community size wind-diesel system and studied voltage and frequency fluctuations. None studied the impact of wind power addition on local load in a community connected to the grid through a long transmission line. In this research two remote communities in Newfoundland and Labrador are identified to study the impact of wind power addition to

their existing power system. Cartwright is in Labrador, which is an isolated community and is now being supplied by a diesel plant. Other remote area is in the North West side of Newfoundland where the community is now supplied by a central power grid through a long transmission line. In this research work we have tried to identify the potential wind resource available in those two areas and determined voltage variation and frequency variation that are expected in the power system after adding wind power to the existing system.

Chapter 3

Mathematical Model of the Wind Energy Conversion System in Cartwright, Labrador

In this chapter, the mathematical modeling of different components, such as wind turbine, synchronous generator, transmission line, transformer and converter in a wind diesel system are presented. After getting the mathematical equations, these equations are solved using SIMULINK along with the system components already available in the Simulink.

3.1 Wind Energy Conversion system

The history of wind energy demonstrates a general evolution from the use of simple, light devices driven by aerodynamic drag forces; to heavy, material-intensive

drag devices; to the increased use of light, material-efficient aerodynamic lift devices in the modern era. Nowadays wind energy is gaining increasing importance throughout the world. The first wind turbine for electricity generation was developed at the beginning of the twentieth century [22]. During the last decade of the nineteenth century world wide wind capacity doubled approximately every three years. Wind energy was the fastest growing energy technology in 1990s. After the wind power boom in California during the mid-1980s, development slowed down significantly in North America [22]. In past few years, wind energy has become a significant electrical source in many utility systems in Canada. Wind energy is now being used to enhance a progressively larger proportion of Canada's electrical requirement. However, compared to some other countries that rely on wind for a much larger piece of their energy such as the Netherlands, Spain, Denmark and Germany, this segment of the Canadian electrical market is still very small. Today, rapid growth is both encouraged and expected due to various government, utility and industry initiatives boosted by the demands of Canadians for a clean, safe, and consistent source of energy.

3.1.1 Types of wind turbine

Wind energy is now used in isolated grid power system or hybrid system and is able to attain some attention. There are various kinds of wind turbines. A particular type of wind turbine is selected depending on the available resource and requirements. Wind turbines can be classified as explained below:

1. According to the size and capacity

    a) Small wind turbine (<300kW)

22

b) Large wind turbine (>300kW)

2. According to rotor speed

    a) Fixed speed wind turbine

    b) Variable speed wind turbine

3. According to rotor axis orientation

    a) Horizontal axis

    b) Vertical axis

Based on load demand and types of power system, different sizes of wind turbines are chosen. Here large wind turbines are chosen to deliver electricity in lower rate. This is due to the cost of foundations, road building, electrical grid connection, different electronic control system which are somewhat independent of the size of the machine. The cost of foundations does not rise in proportion to the size of the machine, and maintenance costs are largely independent of the size of the machine. In areas where it is difficult to find sites for more than a single turbine, a large turbine with a tall tower uses the existing wind resource more efficiently. Small sized wind turbines are chosen most likely to supply power to the local electrical grid which may be very weak to handle the small range of electricity. This may be the case in remote parts of the electrical grid with low population density and little electricity consumption in the area. There is a smaller amount of fluctuation in the output from a wind park consisting of a number of smaller machines since wind fluctuations occur randomly and therefore tend to cancel out. The initial investment for installing a small wind turbine will be much less compared with the larger one.

In the early 1990s the standard installed wind turbines operated at fixed speed. The rotor speed of this kind of wind turbine is determined by the frequency of the supply grid. These wind turbines are designed to achieve maximum efficiency at one particular wind speed. The main advantage of this kind of wind turbine is that they are simple, robust, reliable and lower in cost. Their disadvantages are an uncontrollable reactive power consumption, mechanical stress and limited power quality control. Due to their fixed speed operation wind speed fluctuation also affect the weak power quality with voltage fluctuation, frequency fluctuation etc. So to avoid these problems most of the power companies are now using variable speed wind turbine. These types of wind turbine are used to operate over a wide range of frequency. The electrical system of a variable speed wind turbine is more complicated than a fixed speed wind turbine. The advantage of a variable speed wind turbine is an increased energy capture, improved power quality and reduced mechanical stress.

Horizontal-axis wind turbines (HAWT) have the main rotor shaft and electrical generator at the top of a tower. Most have a gearbox, which turns the slow rotation of the blades into a quicker rotation that is more suitable to drive an electrical generator. There is a variable blade pitch, which gives the turbine blades the optimum angle of attack. So the turbine collects the maximum amount of wind energy for the time of day and season. This type of wind turbine has high efficiency. Because of their tall towers and blades the installation cost can be more. They require additional yaw control system to turn the blades toward the wind. Vertical-axis wind turbines (VAWT) have the main rotor shaft arranged vertically. VAWT can utilize winds from varying directions. They may be built at locations where taller structures are prohibited. They require lower wind speed as

compared with HWAT. Designs without yaw mechanisms are possible with fixed pitch rotor designs. The main disadvantage with this type of turbine is that they produce 50% less energy as compared with HWAT.

3.1.2 Wind Energy Conversion

Most of the grid-connected commercial wind turbines today are built with a propeller-type rotor on a horizontal axis to convert the linear motion of the wind into rotational energy that can be used to drive a generator. Based on speed, fixed-speed wind turbines are the pioneers of the wind turbine industry. They are simple, reliable and use low-cost electrical parts. They use induction generators and they are connected directly to the grid, giving them an almost constant rotor speed stuck to the grid frequency, regardless of the wind speed. In this research work a fixed speed horizontal axis wind turbine was chosen.

Figure 3.1 illustrates the links between the most important components and associated energy conversion stages [23]. Here a fixed speed wind turbine equipped with an induction generator is connected to the grid through transformer and protective devices. The MATLAB/SIMULINK modeling of the wind energy conversion system is discussed through out the following sections.
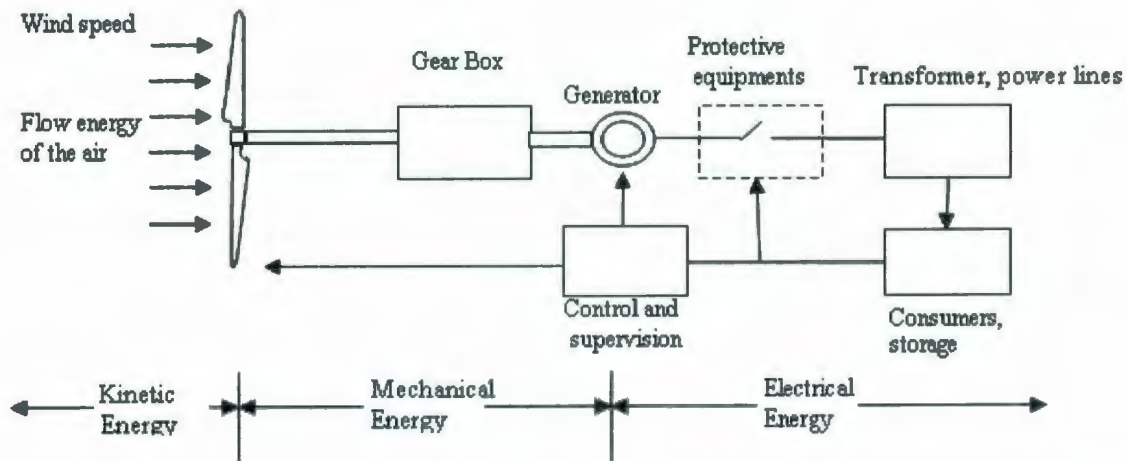
Figure 3.1: Functional chain and conversion stages of wind turbine

The kinetic energy of an air mass m moving at a velocity v can be expressed as

$$E = \frac{1}{2}mv^2 \quad (Nm)$$

Here the mass flow with the air density ρ is:

$$\dot{m} = \rho v A \quad (kg/s)$$

So the energy is physically identical to the power P:

$$P = \frac{1}{2}\rho v^3 A \quad (W)$$

With the help of Betz elementary Momentum theory the typical output characteristic of a wind turbine is given by [24]:

$$P = \frac{1}{2}C_p(\lambda, \alpha)\rho v^3 A \quad (W) \qquad 3.1.1$$

Here ρ (kg/m^3) is the air density, A (m^2) is the rotor swept area and C_p is known as the performance co-efficient which can be expressed as a function of tip speed ratio (λ). Here the tip speed (λ) is obtained from the quotient of the peripheral velocity V_u (rad-m/sec) to the undisturbed wind velocity V_1 (m/s)

$$\lambda = \frac{V_u}{V_1} \qquad\qquad 3.1.2$$

For a fixed blade pitch turbine C_p can be approximately expressed as [24]:

$$Cp = \frac{1}{2} \times \left(\frac{116}{\lambda_p} - 0.4 \times (\alpha - 5) \right) \exp^{\frac{-16.5}{\lambda_p}} \qquad\qquad 3.1.3$$

Here

$$\lambda_p = \frac{1}{\dfrac{1}{(\lambda + 0.089)} - \dfrac{0.035}{\alpha^3 + 1}} \qquad\qquad 3.1.4$$

Where α is the blade pitch angle. For this modeling a mid sized wind turbine was chosen which rated power is 250kw (max. 260kW) at rated rotor speed 32 rpm and at wind speed 13m/s. Here blade pitch angle is assumed to be constant. With the help of above numbered equations the wind turbine is modeled in SIMULINK

3.1.3 Gearbox

The drive power of a wind turbine engenders torques in its mechanical drive train or generator that is subject to fluctuation as a result of both periodic and aperiodic process, such as [23]

a) change in wind speed

b) tower-shadow or tower-occasioned upwind overpressure,

27

c) blade asymmetry,

d) blade bending and skewing and

e) tower oscillation

In addition, load moments in generator due to

a) static

b) dynamic and

c) electromechanical

These behaviors also act on the wind turbine via drive train. The interaction of all torque effects works together with the flywheel-effect-dependent acceleration components to determine conditions in the mechanical drive train. Here the equivalent model of a wind turbine drive train is presented in Figure 3.2. It includes turbine low speed shaft, gear box and generator high speed shaft. Here aerodynamic torque (T_T) is counteracted by the electromechanical torque generated by generator (T_g) through the gear box.
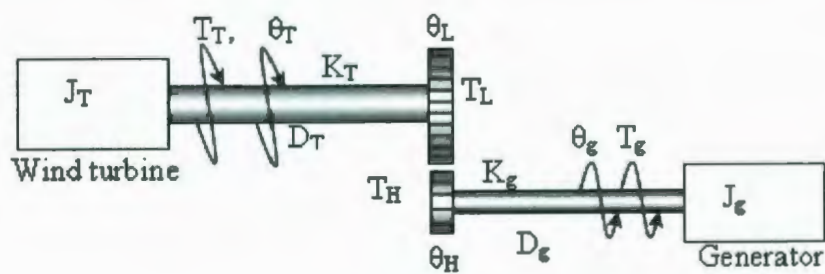

Figure 3.2: Two mass Model of the wind turbine drive train

Here the corresponding torque equations of different stages for the whole model is given by-

$$T_T = J_T \frac{d^2\theta_T}{dt^2} + D_T \frac{d\theta_T}{dt} + K_T(\theta_T - \theta_L)$$

$$T_L = J_{grt} \frac{d^2\theta_L}{dt^2} + D_{grt} \frac{d\theta_L}{dt} + K_{grt}(\theta_L - \theta_T)$$

$$T_H = J_{grg} \frac{d^2\theta_H}{dt^2} + D_{grg} \frac{d\theta_H}{dt} + K_{grg}(\theta_H - \theta_g)$$

$$-T_g = J_g \frac{d^2\theta_g}{dt^2} + D_g \frac{d\theta_g}{dt} + K_g(\theta_g - \theta_H)$$

$$\frac{T_L}{T_H} = gr$$

Where J_T, J_g, D_T, D_g, K_T, K_g are moment of inertia, damping co-efficient, stiffness of wind turbine and generator respectively. T_L is torque into the gear box and T_H is the torque out of the gear box. The model can be reduced to a single mass model [25] by considering high stiffness of wind turbine rotor and generator and also neglecting the moment of inertia, damping co-efficient and stiffness for the gearbox as these are very small compared with the wind turbine rotor and generator. So the torque equation for this simplified model can be given by-

$$T_g - T_T = J_{equ} \times \frac{d^2\theta_G}{dt^2} \qquad\qquad 3.1.5$$

$$J_{equ} = J_G + \frac{J_T}{gr^2} \qquad\qquad 3.1.6$$

Here *gr* is the gear ratio of the gear box. The above equation represents the torque equation for induction machine operating as motor operation. For generator operation the only change is instead of negative sign there will be a positive sign in torque equation [26].

3.1.4 Induction Machine Model

The induction generators commonly used on fixed – speed wind turbines are very similar to conventional industrial induction motors. Figure 3.3 shows a cut away view for a three phase squirrel cage induction machine. The only differences between an induction machine operating as a generator and as a motor are the direction of power flow in the connecting wires, whether torque is applied to or taken from the shaft and the rotor speed is slightly above or below the synchronous speed.
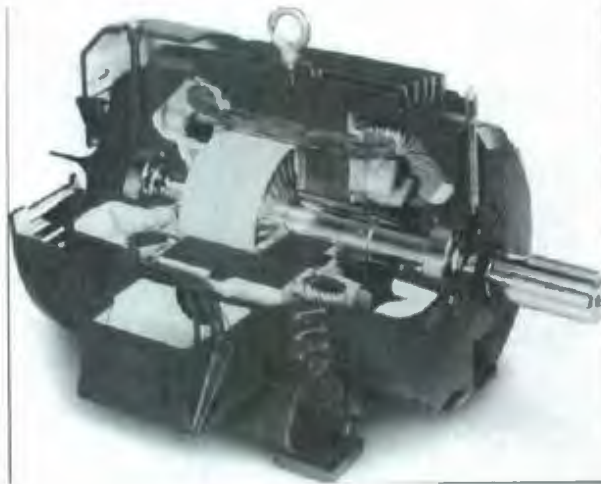
Figure 3.3: Cutaway view of three phase squirrel cage induction machine [27]

The induction machine d - q or dynamic equivalent circuit is shown in Figure 3.4. There are numerous ways of formulating the equations of an induction machine for the purposes of computer simulation. Although the behavior of a symmetrical induction machine may be described in any frame of reference, there are three commonly used: the stationary reference frame, the rotor reference frame and the synchronously rotating

frame. One of the most popular induction motor models derived from this equivalent circuit is Krause's model. According to Krause's model the voltage equations [27] in the arbitrary reference frame may be written as:

$$v_{qds} = R_s i_{qds} + \omega \lambda_{dqs} + p \lambda_{qds}$$
$$v'_{qdr} = R_r i'_{qdr} + (\omega - \omega_r) \lambda'_{dqr} + p \lambda'_{qdr}$$

Where

$$\left(\lambda_{dqs} \right)^T = \begin{bmatrix} \lambda_{ds} & -\lambda_{qs} \end{bmatrix}$$
$$\left(\lambda'_{dqr} \right)^T = \begin{bmatrix} \lambda'_{dr} & -\lambda'_{qr} \end{bmatrix}$$

So the voltage equations in expanded form can be written as:

$$v_{qs} = R_s i_{qs} + \omega \lambda_{ds} + p \lambda_{qs}$$
$$v_{ds} = R_s i_{ds} - \omega \lambda_{qs} + p \lambda_{ds}$$
$$v'_{qr} = R'_r i'_{qr} + (\omega - \omega_r) \lambda'_{dr} + p \lambda'_{qr}$$
$$v'_{dr} = R'_r i'_{dr} - (\omega - \omega_r) \lambda'_{qr} + p \lambda'_{dr}$$

Also the flux linkage equations in expanded form can be written as-

$$\lambda_{qs} = L_{ls} i_{qs} + L_m \left(i_{qs} + i'_{qr} \right)$$
$$\lambda_{ds} = L_{ls} i_{ds} + L_m \left(i_{ds} + i'_{dr} \right)$$
$$\lambda'_{qr} = L'_{lr} i'_{qr} + L_m \left(i_{qs} + i'_{qr} \right)$$
$$\lambda'_{dr} = L'_{lr} i'_{dr} + L_m \left(i_{ds} + i'_{dr} \right)$$

31

q axis

d axis
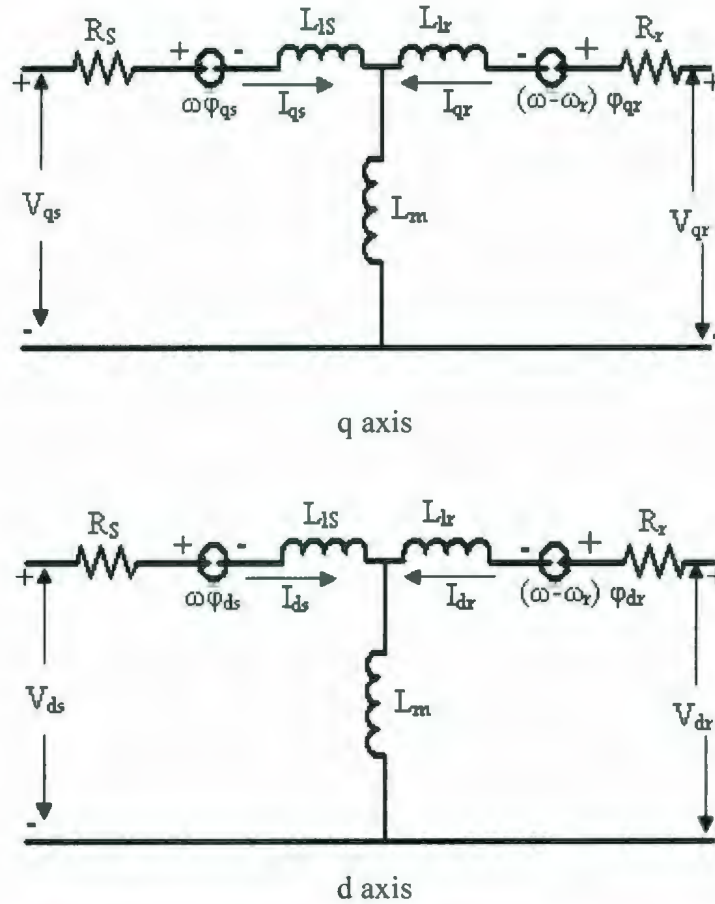
Figure 3.4: d-q axis equivalent circuit of a 3-phase induction machine.

As machine and power system parameters are always given in ohms or percentage, it is convenient to express the above voltages in terms of reactance:

$$v_{qs} = R_s i_{qs} + \frac{\omega}{\omega_b} \varphi_{ds} + \frac{p}{\omega_b} \varphi_{qs}$$

3.1.7

$$v_{ds} = R_s i_{ds} - \frac{\omega}{\omega_b} \varphi_{qs} + \frac{p}{\omega_b} \varphi_{ds}$$

3.1.8

$$v'_{qr} = R'_r i'_{qr} + \left(\frac{\omega - \omega_r}{\omega_b}\right) \varphi'_{dr} + \frac{p}{\omega_b} \varphi'_{qr}$$

3.1.9

$$v'_{dr} = R'_r i'_{dr} - \left(\frac{\omega - \omega_r}{\omega_b}\right) \varphi'_{qr} + \frac{p}{\omega_b} \varphi'_{dr}$$

3.1.10

32

Also the flux linkage equation can be written in terms of reactance as follows.

$$\varphi_{qs} = X_{ls} i_{qs} + X_m \left(i_{qs} + i'_{qr} \right) \qquad\qquad 3.1.11$$

$$\varphi_{ds} = X_{ls} i_{ds} + X_m \left(i_{ds} + i'_{dr} \right) \qquad\qquad 3.1.12$$

$$\varphi'_{qr} = X'_{lr} i'_{qr} + X_m \left(i_{qs} + i'_{qr} \right) \qquad\qquad 3.1.13$$

$$\varphi'_{dr} = X'_{lr} i'_{dr} + X_m \left(i_{ds} + i'_{dr} \right) \qquad\qquad 3.1.14$$

The above equations are convenient for simulating the symmetrical induction machine in the arbitrary reference frame. The above equation can also be used to determine the currents in induction machine windings in the following way:

$$i_{qs} = \frac{1}{X_{ls}} \left(\varphi_{qs} - \varphi_{mq} \right) \qquad\qquad 3.1.15$$

$$i_{ds} = \frac{1}{X_{ls}} \left(\varphi_{ds} - \varphi_{md} \right) \qquad\qquad 3.1.16$$

$$i_{qr} = \frac{1}{X_{lr}} \left(\varphi_{qr} - \varphi_{mq} \right) \qquad\qquad 3.1.17$$

$$i_{dr} = \frac{1}{X_{lr}} \left(\varphi_{dr} - \varphi_{md} \right) \qquad\qquad 3.1.18$$

In the above equation d-axis and q-axis mutual flux quantity can be expressed as:

$$\varphi_{mq} = X_m \left(i_{qs} + i'_{qr} \right)$$

$$\varphi_{md} = X_m \left(i_{ds} + i'_{dr} \right)$$

33

Now if the current quantities in the above equations from 3.1.11 to 3.1.14 can be replaced then the resulting voltage equations from 3.1.7 to 3.1.10 can be solved for the flux linkages per second which are given below:

$$\varphi_{qs} = \omega_b \int \left[v_{qs} - \frac{\omega}{\omega_b} \varphi_{ds} + \frac{R_s}{X_{ls}} \left(\varphi_{mq} - \varphi_{qs} \right) \right] dt \qquad\qquad 3.1.19$$

$$\varphi_{ds} = \omega_b \int \left[v_{ds} + \frac{\omega}{\omega_b} \varphi_{qs} + \frac{R_s}{X_{ls}} \left(\varphi_{md} - \varphi_{ds} \right) \right] dt \qquad\qquad 3.1.20$$

$$\varphi'_{qr} = \omega_b \int \left[v'_{qr} - \frac{\omega - \omega_r}{\omega_b} \varphi'_{dr} + \frac{R'_r}{X'_{lr}} \left(\varphi_{mq} - \varphi'_{qr} \right) \right] dt \qquad\qquad 3.1.21$$

$$\varphi'_{dr} = \omega_b \int \left[v'_{dr} + \frac{\omega - \omega_r}{\omega_b} \varphi'_{qr} + \frac{R'_r}{X'_{lr}} \left(\varphi_{md} - \varphi'_{dr} \right) \right] dt \qquad\qquad 3.1.22$$

As squirrel cage induction machine is used, V'_{dr} and V'_{qr} in above equations are set to zero. So the magnetizing flux equation can be written in following ways:

$$\varphi_{mq} = X_t \left(\frac{\varphi_{qs}}{X_{ls}} + \frac{\varphi'_{qr}}{X'_{lr}} \right) \qquad\qquad 3.1.23$$

$$\varphi_{md} = X_t \left(\frac{\varphi_{ds}}{X_{ls}} + \frac{\varphi'_{dr}}{X'_{lr}} \right) \qquad\qquad 3.1.24$$

Where

$$X_t = \left(\frac{1}{X_m} + \frac{1}{X_{ls}} + \frac{1}{X'_{lr}} \right)^{-1} \qquad\qquad 3.1.25$$

34

The electromagnetic torque equation can be given by

$$T_g = \frac{3P}{4\omega_b}\left(\varphi_{ds}i_{qs} - \varphi_{qs}i_{ds}\right)$$

3.1.26

With the help of equations 3.1.7 to 3.1.26 the wind energy conversion system can be modeled in SIMULINK. The sub-systems are given in Appendix A.

3.2   Transformer

The power transformer is a major power system component that permits economical power transmission with high efficiency and low series voltage drops. The main uses of electrical transformers are for changing the magnitude of an ac voltage, providing electrical isolation and matching the impedance of the load to the source. For an ideal transformer it is assumed the windings have zero resistance, the core permeability is infinite, there is no leakage flux and there are no core losses [28]. A schematic representation of a two winding transformer is shown in figure 3.5
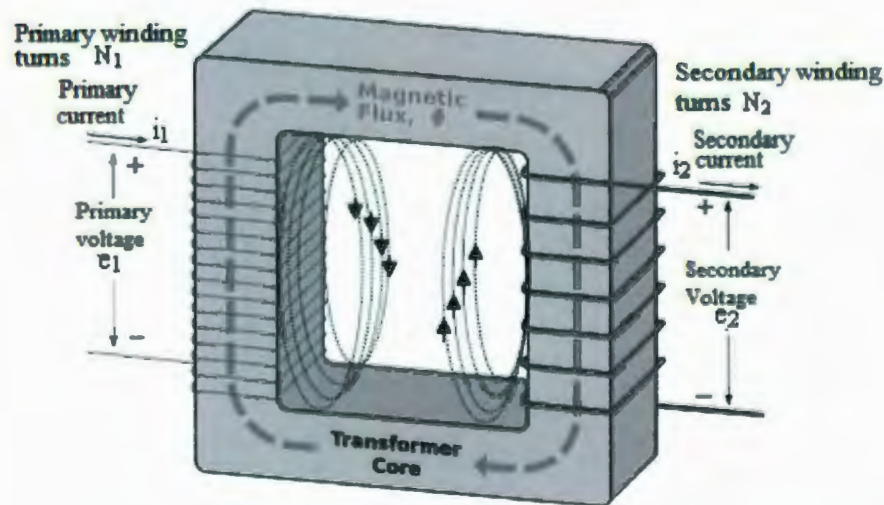

Figure 3.5: Diagram of a single phase two winding transformer. [28]

With the core reluctance neglected, the resultant mmf needed to magnetize the core is zero. That is

$$N_1 i_1 = -N_2 i_2$$

$$\frac{N_1}{N_2} = -\frac{i_2}{i_1}$$

The induced voltage in the winding is:

$$e_1 = N_1 \frac{d\varphi_m}{dt} \quad \& \quad e_2 = N_2 \frac{d\varphi_m}{dt}$$

$$\frac{e_1}{e_2} = \frac{N_1}{N_2}$$

If there is no power loss in the transformer, then the net power flow into the ideal transformer from both of its windings will be zero.

$$e_1 i_1 = \frac{N_1}{N_2} e_2 \times \left(-i_2 \frac{N_2}{N_1} \right) = -i_2 e_2$$

In the above equation the positive polarity of the voltages is on one side of the winding and the direction of the currents is into the winding. For simulating and analyzing, circuit variables on one side can be transferred to other side to obtain the simpler equivalent circuit. Transferring one side variables to other side can be done by

$$Z_1 = \frac{e_1}{i_1} = \frac{N_1}{N_2} e_2 \left(-\frac{1}{i_2} \cdot \frac{N_1}{N_2} \right) = -\left(\frac{N_1}{N_2} \right)^2 \frac{e_2}{i_2} = \left(\frac{N_1}{N_2} \right)^2 z_2$$

From figure 3.6 it can be seen that there are two components of flux of each winding: mutual components which link both windings and leakage flux component which links only the circuit itself. So the total flux linked by each winding can be given by:

$$\varphi_1 = \varphi_{l_1} + \varphi_m \qquad\qquad 3.2.1$$

$$\varphi_2 = \varphi_{l_2} + \varphi_m \qquad\qquad 3.2.2$$

Here φ_{l_1} and φ_{l2} are the leakage flux components of winding 1 and 2 respectively. For an ideal transformer, the mutual flux is established by the resultant mmf of the two windings acting around the same core. The flux linkage of the winding 1 can be given by

$$\lambda_1 = N_1 \varphi_1 = N_1 \left(\varphi_{l_1} + \varphi_m \right)$$

Here

$$\varphi_{l_1} = N_1 i_1 \mu_{l_1} \qquad\qquad 3.2.3$$

$$\varphi_m = \left(N_1 i_1 + N_2 i_2 \right) \mu_m \qquad\qquad 3.2.4$$

Here μ_{l_1} is the leakage path permeance of winding 1 and μ_m is the mutual path permeance. The above flux linkage equation can be expressed in terms of the winding currents by replacing leakage and mutual fluxes by their respective mmf and permeance. So for winding 1 flux linkage equation can be written as follows:

37

$$\lambda_1 = N_1\left(N_1 i_1 \mu_{l_1} + (N_1 i_1 + N_2 i_2)\mu_m\right) = \left(N_1^2 \mu_{l_1} + N_1^2 \mu_m\right)i_1 + N_1 N_2 i_2 \mu_m$$

Similarly for winding 2

$$\lambda_2 = \left(N_2^2 \mu_{l_2} + N_2^2 \mu_m\right)i_2 + N_1 N_2 i_1 \mu_m$$

The resulting flux linkage equations for the two magnetically coupled windings can be expressed in terms of winding inductances as follows:

$$\lambda_2 = L_{21} i_1 + L_{22} i_2 \qquad\qquad 3.2.5$$

$$\lambda_1 = L_{11} i_1 + L_{12} i_2 \qquad\qquad 3.2.6$$

Here the self inductances of winding 1 and 2 can be expressed in terms of their magnetizing and self inductances which are given below:

$$L_{11} = \frac{(\lambda_1)_{i_2=0}}{i_1} = \overbrace{N_1^2 \mu_{l_1}}^{L_{l_1}} + \overbrace{N_1^2 \mu_m}^{L_{m1}}$$

$$L_{22} = \frac{(\lambda_2)_{i_1=0}}{i_2} = \overbrace{N_2^2 \mu_{l_2}}^{L_{l_2}} + \overbrace{N_2^2 \mu_m}^{L_{m2}}$$

The equivalent circuit representation of a two winding transformer is shown in figure 3.6. The above figure shows the transformer has winding resistances, infinite core permeability, magnetic flux is not entirely confined to the core and there are real and reactive power losses in the core.
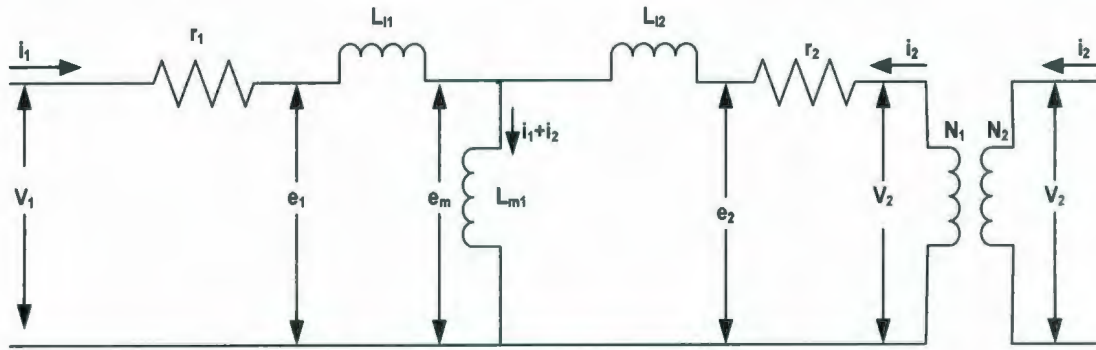
Figure 3.6: Equivalent circuit of a two winding transformer

The induced voltage in each winding is equal to the rate of change of the winding's flux linkage. So the induced voltage in winding 1 is:

$$e_1 = \frac{d\lambda_1}{dt} = \frac{d}{dt}\left\{L_{11}i_1 + i_2 L_{12}\right\}$$

$$= \frac{d}{dt}\left\{\left(L_{m_1} + L_{l_1}\right)i_1 + \frac{N_2}{N_1}L_{m_1}i_2\right\}$$

$$= L_{l_1}\frac{di_1}{dt} + L_{m_1}\frac{d}{dt}\left(i_1 + i_2'\right)$$

Similarly the induced voltage in winding 2 is

$$e_2 = L_{l_2}\frac{di_2}{dt} + L_{m_2}\frac{d}{dt}\left(\frac{N_1}{N_2}i_1 + i_2\right) \qquad 3.2.7$$

To make a simplified calculation it is required to transfer the voltage e_2 to winding 1 which is given below

$$e_1 = \frac{N_1}{N_2}e_2$$

$$\frac{N_1}{N_2}e_2 = \frac{N_1}{N_2}L_{l_2}\frac{di_2}{dt} + L_{m_2}\frac{N_1}{N_2}\frac{d}{dt}\left(\frac{N_1}{N_2}i_1 + i_2\right)$$

$$e_2' = L_{l_2}'\frac{di_2}{dt} + L_{m_2}\left(\frac{N_1}{N_2}\right)^2\frac{d}{dt}\left(i_1 + \frac{N_2}{N_1}i_2\right)$$

$$e_2' = L_{l_2}'\frac{di_2}{dt} + L_{m_1}\frac{d}{dt}\left(i_1 + i_2'\right) \qquad\qquad 3.2.8$$

The flux linkage and winding currents can be used to represent winding voltages as follows:

$$V_1 = i_1 R_1 + \frac{d\lambda_1}{dt} = i_1 R_1 + \frac{1}{\omega_b}\frac{d\varphi_1}{dt} \qquad\qquad 3.2.9$$

Similarly for winding 2:

$$V_2' = i_2'R_2' + \frac{1}{\omega_b}\frac{d\varphi_2'}{dt} \qquad\qquad 3.2.10$$

Here

$$\varphi_1 = \omega_b\lambda_1 = X_{l_1}i_1 + \omega_b\varphi_m$$

$$\varphi_2' = \omega_b\lambda_2' = X_{l_2}'i_2' + \omega_b\varphi_m$$

Where

$$\varphi_m = \omega_b L_{m_1}\left(i_1 + i_2'\right)$$

So the current equations are

$$i_1 = \frac{\varphi_1 - \varphi_m}{X_{l_1}} \quad and \quad i_2' = \frac{\varphi_2' - \varphi_m}{X_{l_2}'} \qquad\qquad 3.2.11$$

40

$$\therefore \varphi_m = X_{m_1} \left(\frac{\varphi_1 - \varphi_m}{X_{l_1}} + \frac{\varphi_2' - \varphi_m}{X_{l_2}'} \right)$$

$$\varphi_m \left(\frac{1}{X_{m_1}} + \frac{1}{X_{l_1}} + \frac{1}{X_{l_2}'} \right) = \frac{\varphi_1}{X_{l_1}} + \frac{\varphi_2'}{X_{l_2}'}$$

$$\varphi_m = X_m \left(\frac{\varphi_1}{X_{l_1}} + \frac{\varphi_2'}{X_{l_2}'} \right) \qquad\qquad 3.2.12$$

Where

$$\frac{1}{X_m} = \frac{1}{X_{m_1}} + \frac{1}{X_{l_1}} + \frac{1}{X_{l_2}'} \qquad\qquad 3.2.13$$

From equation 3.2.9 it was found that:

$$V_1 = i_1 R_1 + \frac{1}{\omega_b} \frac{d\varphi_1}{dt}$$

$$\frac{d\varphi_1}{dt} = \omega_b (V_1 - i_1 R_1) = \omega_b \left[V_1 - R_1 \left(\frac{\varphi_1 - \varphi_m}{X_{l_1}} \right) \right]$$

$$\varphi_1 = \omega_b \int \left[V_1 - R_1 \left(\frac{\varphi_1 - \varphi_m}{X_{l_1}} \right) \right] dt \qquad\qquad 3.2.14$$

Similarly for winding -2, flux linkage equation can be written as:

$$\varphi_2 = \omega_b \int \left[V_2' - R_2' \left(\frac{\varphi_2' - \varphi_m}{X_{l_2}'} \right) \right] dt \qquad\qquad 3.2.15$$

With the help of equation from 3.2.1 to 3.2.15 the transformer can be modeled in SIMULINK. The sub-systems are given in Appendix A.

41

3.3 Transmission Line

Electric power transmission is the bulk transfer of electrical power, a process in the delivery of electricity to consumers. A power transmission network typically connects power plants to multiple substations near a populated area. Usually transmission lines use three phase alternating current (AC). Single phase AC current is sometimes used in a railway electrification system. High-voltage direct current systems are used for long distance transmission, or some undersea cables, or for connecting two different ac networks. Electricity is transmitted at high voltages (110 kV or above) to reduce the energy lost in transmission. Power is usually transmitted as alternating current through overhead power lines [29].

Overhead conductors are not covered by insulation. Improved conductor material and shapes are regularly used to allow increased capacity and modernize transmission circuits. Today, transmission-level voltages are usually considered to be 110 kV and above [30]. Lower voltages such as 66 kV and 33 kV are usually considered sub-transmission voltages but are occasionally used on long lines with light loads. Voltages less than 33 kV are usually used for distribution. Voltages above 230 kV are considered extra high voltage and require different designs compared to equipment used at lower voltages.

A single phase of a balanced three phase transmission line can be represented by figure 3.7. The impedances and admittances of the transmission line are considered to be uniformly distributed [28]. Here in figure 3.7 a very small length Δx of transmission is considered.
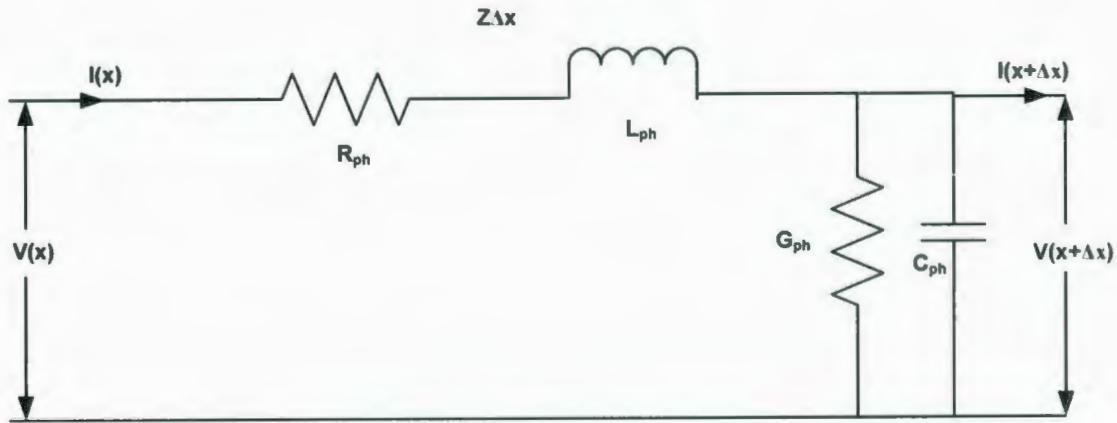
Figure 3.7: Schematic diagram of a single phase transmission line

In the above figure $Z\Delta x$ is the series impedance of the elemental length of the line and $y\Delta x$ is the shunt admittance. The voltage at the sending end is V(x) and receiving end is V(x+Δx). Applying KVL around the elemental loop the voltage equation can be found as follows [29]:

$$V(x) = I(x)Z\Delta x + V(x + \Delta x)$$

$$\frac{V(x) - V(x + \Delta x)}{\Delta x} = I(x)Z$$

If $\Delta x \rightarrow 0$

$$-\frac{\partial V}{\partial x} = \left(Ri + L\frac{\partial i}{\partial t} \right) \qquad 3.3.1$$

Applying KCL current equation can be found as follows [29]

$$I(x) = V(x + \Delta x)Y\Delta x + I(x + \Delta x)$$

$$\frac{I(x) - I(x + \Delta x)}{\Delta x} = V(x + \Delta x)Y$$

Letting $\Delta x \rightarrow 0$

$$-\frac{\partial i}{\partial x} = \left(Gv + C\frac{\partial v}{\partial t} \right) \qquad 3.3.2$$

The equation 3.3.1 and 3.3.2 are the function of x and time t. Applying Laplace transforms and ignoring the initial condition differential equation of voltage and current be found as [29]:

$$V(s) = \frac{dV}{dx} = -(R + sL)I = -ZI$$

$$I(s) = \frac{dI}{dx} = -(G + sC)V = -YV$$

Again differentiating, it is found that:

$$\frac{d^2I}{dx^2} = -(G + sC)\frac{dV}{dx} = (G + sC)(R + sL)I$$

$$\frac{d^2I}{dx^2} = (G + sC)(R + sL)I$$

Similarly voltage equation can be found that:

$$\frac{d^2V}{dx^2} = (G + sC)(R + sL)V$$

Taking the solution of above equation it is found that

$$I(x,s) = A_1 e^{\gamma x} + A_2 e^{-\gamma x}$$

$$V(x,s) = \underbrace{-Z_c A_1 e^{\gamma x}}_{V_b} + \underbrace{Z_c A_2 e^{-\gamma x}}_{V_f}$$

44

In the above equations, γ is known as propagation constant and Z_c is known as characteristic impedance of the line.

$$\gamma = \sqrt{(R + sL)(G + sC)} \qquad\qquad 3.3.3$$

$$Z_c = \sqrt{\frac{(R + sL)}{(G + sC)}} \qquad\qquad 3.3.4$$

Here

$$V_f = I_f Z_c \ \ and \ \ V_b = -I_b Z_c$$

so

$$V(x,s) = V_f + V_b$$

If the line is terminated by some impedance $Z_d(s)$ at the receiving end then:

$$Z_d(s) = \frac{V(d,s)}{I(d,s)} = \frac{Z_c(I_f - I_b)}{I_b + I_f} = \frac{Z_c I_f\left(1 - \dfrac{I_b}{I_f}\right)}{I_f\left(1 + \dfrac{I_b}{I_f}\right)} = \frac{Z_c(1 - \rho_i)}{(1 + \rho_i)}$$

$$\frac{Z_d}{Z_c} = \frac{1 - \rho_i}{1 + \rho_i}$$

Where ρ_i = current reflection co-efficient. $= \dfrac{Z_c - Z_d}{Z_c + Z_d}$

And ρ_v = Voltage reflection co-efficient $= \dfrac{V_b}{V_f} = \dfrac{Z_d - Z_c}{Z_d + Z_c} = -\rho_i$

The integration constants A_1 and A_2 are the functions of the boundary conditions. Setting

x = d

$$\rho_i = \frac{i_b(d)}{i_f(d)} = \frac{A_1 e^{\gamma d}}{A_2 e^{-\gamma d}} = \frac{A_1}{A_2} e^{2\gamma d}$$

Again it is known that, $i(x,s) = A_1 e^{\gamma x} + A_2 e^{-\gamma x}$

At x = 0

$$i(0,s) = A_1 + A_2$$

$$A_1 = \frac{I(0,s)\rho_i e^{-2\gamma d}}{1 + \rho_i e^{-2\gamma d}}$$

$$A_2 = \frac{I(0,s)}{1 + \rho_i e^{-2\gamma d}}$$

If d → α, $A_1 = 0$ and $A_2 = $ i (o, s). So the current equation can be written as:

$$I(x,s) = I(0,s)e^{-\gamma x}$$

Using Taylor's expansion of γ it is found that

$$\gamma = \frac{R}{2}\sqrt{\frac{C}{L}} + s\sqrt{LC} = \alpha + s\beta$$

Taking the inverse Laplace of the current equation it is found that

$$I(x,t) = e^{-\frac{R}{2}\sqrt{\frac{C}{L}}x} I\left(0, t - \sqrt{LC}x\right) u\left(t - \sqrt{LC}x\right)$$

So

$$V(x,t) = Z_c I(x,t)$$

The time taken by a wave to cover a distance 'd' can be given by

$$\Gamma = d\sqrt{LC} \qquad\qquad 3.3.5$$

46

When the switch is closed, applying a voltage to a line a voltage wave accompanied by a wave current starts to travel along the line. Here figure 3.8 shows that a load is connected to a source through a distributed transmission line.
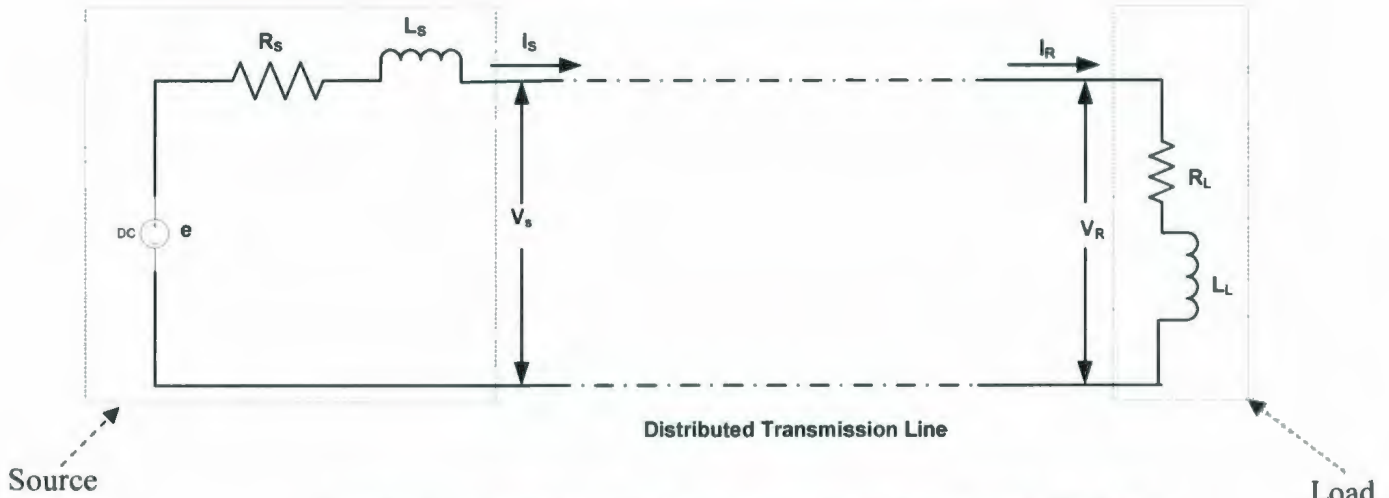

Figure 3.8: A single phase line connecting a source to an RL load

To calculate the sending end current, KVL is applied in the source side which is given below

$$e = V_s + I_s R_s + L_s \frac{dI_s}{dt}$$

$$I_s = \frac{1}{L_s} \int (e - V_s - R_s I_s) dt \qquad 3.3.6$$

Similarly to get the receiving end current KVL is applied in the load end side.

$$V_R = I_R R_L + L_L \frac{dI_R}{dt}$$

$$I_R = \frac{1}{L_L} \int (V_R - R_L I_R) dt \qquad 3.3.7$$

47

With a distributed transmission line representation, the voltage and current on the line at any time consists of its forward and backward components. So the sending end voltage can be represented as follows [29]:

$$V_s = V_{fs} + V_{bs}$$
$$V_s = Z_c I_s + 2V_{bs}$$

3.3.8

Similarly on the receiving end side, the voltage can be represented as [29]:

$$V_R = V_{fR} + V_{bR}$$
$$= 2V_{fR} - I_{fR} Z_c$$

3.3.9

With the help of equations from 3.3.3 to 3.3.9 the transmission line can be modeled in SIMULINK. The sub-systems are given in Appendix A.

3.4 Synchronous machine

A "synchronous" generator runs at a constant speed and draws its excitation from a power source external or independent of the load or transmission network it is supplying. A synchronous generator has an exciter that enables the synchronous generator to produce its own reactive power and to also regulate its voltage. Synchronous generators can operate in parallel with the utility or in "stand-alone" or "island" mode. Synchronous generators require a speed reduction gear [31].

Synchronous generators can be readily operated in parallel, and, in fact, the electricity supply systems of industrialized countries typically have scores or even hundreds of them operating in parallel, interconnected by thousands of miles of

48

transmission lines, and supplying electric energy to loads scattered over areas of many thousands of square miles. These huge systems have grown in spite of the necessity for designing the system so that synchronism is maintained following disturbances and the problems, both technical and administrative, which must be solved to coordinate the operation of such a complex system of machines and personnel. When a synchronous generator is connected to a large interconnected system containing many other synchronous generators, the voltage and frequency at its armature terminals are substantially fixed by the system [31].

This section will discuss about the mathematical model of an ideal synchronous machine. The fields produced by the winding currents are assumed to be sinusoidally distributed around the air gap. The rotor reference frame (Park's equation) is used to establish the machine equation to represent the machine for mathematical modelling and simulation. Figure 3.9 shows a d-q representation of a 3-phase synchronous machine [27]. The stator windings are identical sinusoidally distributed windings. The rotor is equipped with a field winding and three short circuited damper windings.


q axis

49
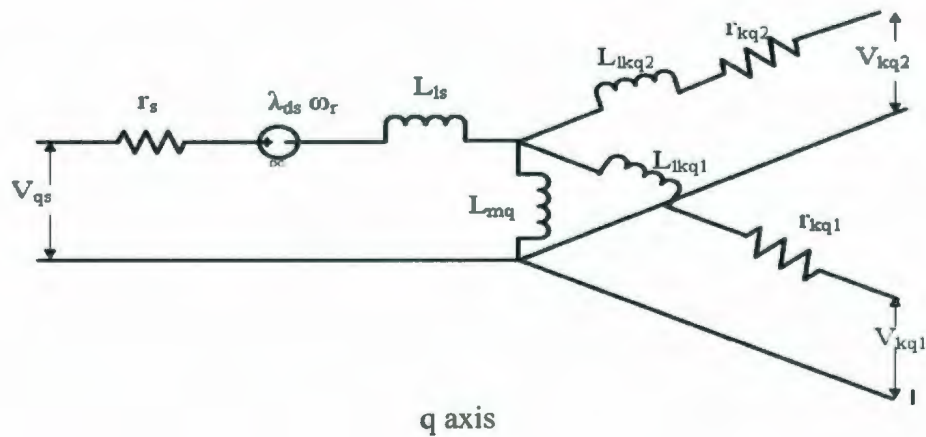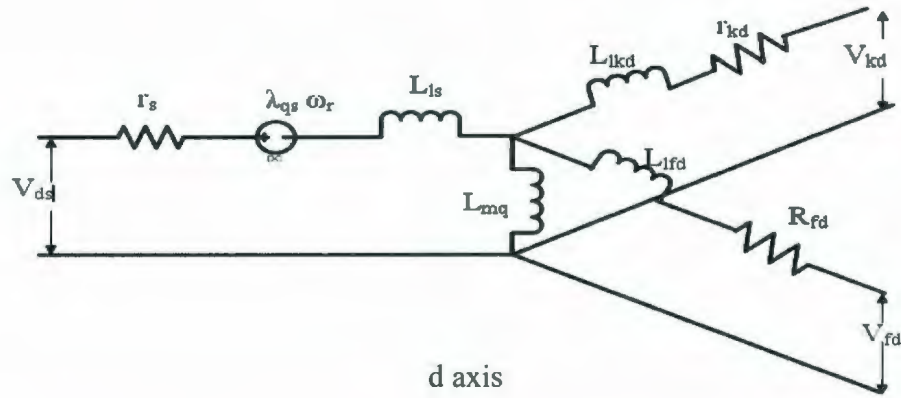
Figure 3.9: d-q representation of a 3-phase synchronous machine

Park transformed the stator variables to the rotor reference frame that eliminates time varying inductances in the voltage equations. So according to his model stator and rotor voltage equation can be represented in rotor reference in the following way [27]:

$$v_{qds} = -R_s i^r_{qds} + \omega \lambda^r_{dqs} + p\lambda^r_{qds}$$
$$v^{/}_{qdr} = R^{/}_r i^{/r}_{qdr} + p\lambda^{/r}_{qdr}$$

Where

$$\left(\lambda^r_{qds}\right)^T = \begin{bmatrix} \lambda^r_{ds} & -\lambda^r_{qs} \end{bmatrix}$$

The d-axis is aligned with the magnetic axis of the rotor field winding and the q-axis is assumed 90° ahead of the d-axis in the direction of rotor speed. Park's voltage equation can be written in expanded form as follows:

$$v^r_{qs} = -R_s i^r_{qs} + \frac{\omega_r}{\omega_b}\varphi^r_{ds} + \frac{p}{\omega_b}\varphi^r_{qs}$$

3.4.1

$$v^r_{ds} = -R_s i^r_{ds} - \frac{\omega_r}{\omega_b}\varphi^r_{qs} + \frac{p}{\omega_b}\varphi^r_{ds}$$

3.4.2

50

$$v_{kq1}^{/r} = R_{kq1}i_{kq1}^{/r} + \frac{p}{\omega_b}\varphi_{kq1}^{/r}$$ 3.4.3

$$v_{kq2}^{/r} = R_{kq2}i_{kq2}^{/r} + \frac{p}{\omega_b}\varphi_{kq2}^{/r}$$ 3.4.4

$$v_{fd}^{/r} = R_{fd}i_{fd}^{/r} + \frac{p}{\omega_b}\varphi_{fd}^{/r}$$ 3.4.5

$$v_{kd}^{/r} = R_{kd}i_{kd}^{/r} + \frac{p}{\omega_b}\varphi_{kd}^{/r}$$ 3.4.6

The currents and flux linkages are related and cannot be independent variables. For computer simulation, it is desirable to express the voltage equations in terms of either currents or flux linkages. Krause [27] suggest taking the flux linkages as the independent variables and then to calculate the currents. The flux linkage equation can be written in terms of reactance we get

$$\varphi_{qs}^{r} = -X_{ls}i_{qs}^{r} + X_{mq}\left(-i_{qs}^{r} + i_{kq1}^{/r} + i_{kq2}^{/r}\right)$$ 3.4.7

$$\varphi_{ds}^{r} = -X_{ls}i_{ds}^{r} + X_{md}\left(-i_{ds}^{r} + i_{fd}^{/r} + i_{kd}^{/r}\right)$$ 3.4.8

$$\varphi_{kq1}^{/r} = X_{lkq1}i_{kq1}^{r} + X_{mq}\left(-i_{qs}^{r} + i_{kq1}^{/r} + i_{kq2}^{/r}\right)$$ 3.4.9

$$\varphi_{kq2}^{/r} = X_{lkq2}i_{kq2}^{r} + X_{mq}\left(-i_{qs}^{r} + i_{kq1}^{/r} + i_{kq2}^{/r}\right)$$ 3.4.10

$$\varphi_{kd}^{/r} = X_{lkd}i_{kd}^{r} + X_{md}\left(-i_{ds}^{r} + i_{fd}^{/r} + i_{kd}^{/r}\right)$$ 3.4.11

$$\varphi_{fd}^{/r} = X_{lfd}i_{fd}^{r} + X_{md}\left(-i_{ds}^{r} + i_{fd}^{/r} + i_{kd}^{/r}\right)$$ 3.4.12

The simulation used most widely is derived from the voltage equations expressed in the rotor reference frame. Expressing the d-q axis voltage equations as integral

equations of the flux linkages of the windings, the above voltage equations along with other inputs can be used in the integral equations to solve for the flux linkages of the windings as follows [27].

$$\varphi_{qs}^{r} = \omega_b \int \left[v_{qs}^{r} - \frac{\omega_r}{\omega_b} \varphi_{ds}^{r} + \frac{R_s}{X_{ls}} \left(\varphi_{mq}^{r} - \varphi_{qs}^{r} \right) \right] dt \qquad 3.4.13$$

$$\varphi_{ds}^{/r} = \omega_b \int \left[v_{ds}^{r} + \frac{\omega_r}{\omega_b} \varphi_{qs}^{r} + \frac{R_s}{X_{ls}} \left(\varphi_{md}^{r} - \varphi_{ds}^{r} \right) \right] dt \qquad 3.4.14$$

$$\varphi_{kq1}^{/r} = \omega_b \int \left[v_{kq1}^{/r} + \frac{R_{kq1}^{/}}{X_{lkq1}} \left(\varphi_{mq}^{r} - \varphi_{kq1}^{/r} \right) \right] dt \qquad 3.4.15$$

$$\varphi_{kq2}^{/r} = \omega_b \int \left[v_{kq2}^{/r} + \frac{R_{kq2}^{/}}{X_{lkq2}} \left(\varphi_{mq}^{r} - \varphi_{kq2}^{/r} \right) \right] dt \qquad 3.4.16$$

$$\varphi_{fd}^{/r} = \omega_b \int \left[\frac{R_{fd}^{/}}{X_{md}} e_{xfd}^{/r} + \frac{R_{fd}^{/}}{X_{lfd}} \left(\varphi_{md}^{r} - \varphi_{fd}^{/r} \right) \right] dt \qquad 3.4.17$$

$$\varphi_{kd}^{/r} = \omega_b \int \left[v_{kd}^{/r} + \frac{R_{kd}^{/}}{X_{lkd}} \left(\varphi_{md}^{r} - \varphi_{kd}^{/r} \right) \right] dt \qquad 3.4.18$$

The salient effect of the generator is taken into account by considering different values of the mutual reactance in the d-q axis. To handle all the set of inductors in d-q axis, all the mutual flux linkages are expressed in terms of the total flux linkages of the winding as follows:

$$\varphi_{mq}^{r} = X_{aq}\left(\frac{\varphi_{qs}^{r}}{X_{ls}} + \frac{\varphi_{kq1}^{\prime r}}{X_{lkq1}^{\prime}} + \frac{\varphi_{kq2}^{\prime r}}{X_{lkq2}^{\prime}}\right) \qquad 3.4.19$$

$$\varphi_{md}^{r} = X_{ad}\left(\frac{\varphi_{ds}^{r}}{X_{ls}} + \frac{\varphi_{fd}^{\prime r}}{X_{lfd}^{\prime}} + \frac{\varphi_{lkd}^{\prime r}}{X_{lkd}^{\prime}}\right) \qquad 3.4.20$$

Where

$$X_{aq} = \left(\frac{1}{X_{mq}} + \frac{1}{X_{ls}} + \frac{1}{X_{lkq1}^{\prime}} + \frac{1}{X_{lkq2}^{\prime}}\right)^{-1} \qquad 3.4.21$$

$$X_{ad} = \left(\frac{1}{X_{md}} + \frac{1}{X_{ls}} + \frac{1}{X_{lkd}^{\prime}} + \frac{1}{X_{lfd}^{\prime}}\right)^{-1} \qquad 3.4.22$$

After calculating the values of the flux linkages of the windings and mutual flux linkages in d-q axis, currents in those axes can be calculated by using the following equations [27]:

$$i_{qs}^{r} = -\frac{1}{X_{ls}}\left(\varphi_{qs}^{r} - \varphi_{mq}^{r}\right) \qquad 3.4.23$$

$$i_{ds}^{r} = -\frac{1}{X_{ls}}\left(\varphi_{ds}^{r} - \varphi_{md}^{r}\right) \qquad 3.4.24$$

$$i_{kq1}^{\prime r} = -\frac{1}{X_{kq1}^{\prime}}\left(\varphi_{kq1}^{\prime r} - \varphi_{mq}^{r}\right) \qquad 3.4.25$$

$$i_{kq2}^{\prime r} = -\frac{1}{X_{kq2}^{\prime}}\left(\varphi_{kq2}^{\prime r} - \varphi_{mq}^{r}\right) \qquad 3.4.26$$

$$i_{fd}^{\prime r} = -\frac{1}{X_{lfd}^{\prime}}\left(\varphi_{fd}^{\prime r} - \varphi_{md}^{r}\right) \qquad 3.4.27$$

$$i_{kd}^{\prime r} = -\frac{1}{X_{lkd}^{\prime}}\left(\varphi_{kd}^{\prime r} - \varphi_{md}^{r}\right) \qquad 3.4.28$$

53

The electromagnetic torque generated by a synchronous machine with P pole can be given by [27]:

$$T_g = \frac{3P}{4\omega_b}\left(\varphi_{ds}\, i_{qs} - \varphi_{qs}\, i_{ds}\right)$$

3.4.29

The synchronous rotor speed can be given by the following equation [27]:

$$\omega_r = -\frac{\omega_b}{2J}\int\left(T_g - T_m\right)dt$$

3.4.30

With the help of equations 3.4.1 to 3.4.30 a synchronous generator is modeled in SIMULINK. The sub-systems are given in Appendix A.

3.5 Converter

Power electronic converters have been one of the fastest growing markets in the electronics industry over the last 25 years. The main application areas for power electronics are in power quality and protection, switch-mode power conversion, batteries and portable power sources, automotive electronics and solar energy technology. As energy is mostly transported on AC lines, electronic circuits able to convert AC to DC voltages have been the first application ever for power semiconductor devices. At large power levels, energy is transported and distributed within three phase systems, and conversion from three-phase AC to DC voltage is used.

A circuit of the load commutated converter is shown in figure 3.10. The converter is fed by three phase ac source with commutating inductance. The circuit also includes a dc inductor and dc resistor which may represent the armature resistance and inductance

of a dc machine or a filtering circuit. The output voltage is the pure dc voltage to be applied to fielding winding or a capacitor voltage in a filter.
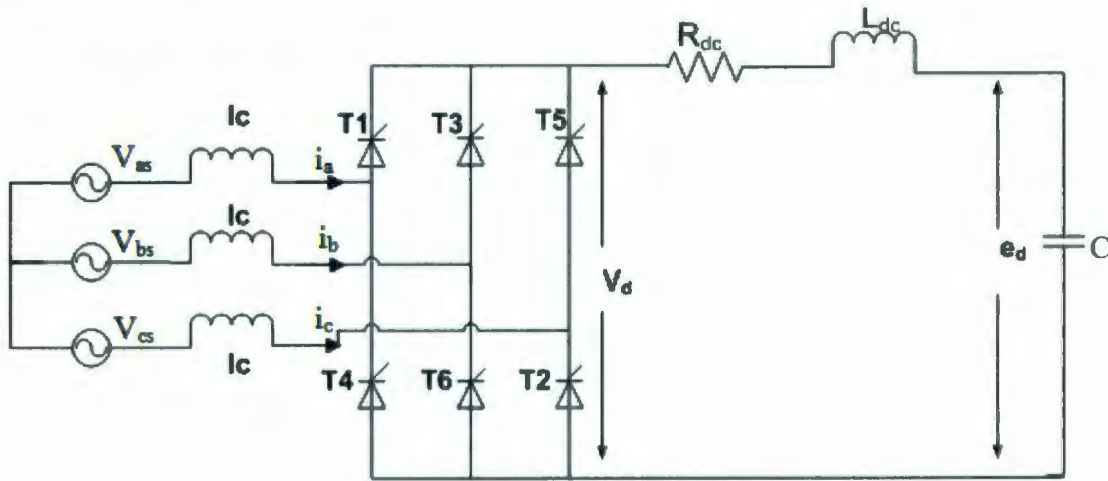

Figure 3.10: Three phase full converter circuit

Three-phase controlled rectifiers have a wide range of applications, from small rectifiers to large high voltage direct current transmission systems. In this figure the converter consists of six gate of a thyristor, the thyristor is said to be gated on, regardless of whether or not it conducts. The AC source voltage may be expressed as [33]:

$$V_{as} = \sqrt{2}ECos\theta + lc\frac{di_a}{dt} \qquad 3.5.1$$

$$V_{bs} = \sqrt{2}ECos\left(\theta - \frac{2\pi}{3}\right) + lc\frac{di_b}{dt} \qquad 3.5.2$$

$$V_{cs} = \sqrt{2}ECos\left(\theta + \frac{2\pi}{3}\right) + lc\frac{di_c}{dt} \qquad 3.5.3$$

The average values may be established for any $\pi/3$ interval of θ. The average dc voltage over this interval may be expressed as

$$V_d = \frac{3}{\pi} \int_{\frac{\pi}{3}+\alpha}^{\frac{2\pi}{3}+\alpha} (V_b - V_c)d\theta + \frac{3}{\pi} l_c \omega \, (i_b - i_c)_{\frac{\pi}{3}+\alpha}^{\frac{2\pi}{3}+\alpha} \qquad 3.5.4$$

In the figure 3.10 the thyristor T_3 begins to conduct only when T_1 & T_2 are conducting. So

$$i_{abc} = [\, -i_d \qquad o \qquad i_d \,]^T$$

Again T_4 begins to conduct only when T_2 & T_3 are on.

$$iabc = [o \qquad -i_d - \Delta i_d \qquad i_d + \Delta i_d]^T$$

In the above equation Δi_d represents the change in average dc current over the given conduction interval due to long term dynamics.

$$\Delta i_d = \frac{\pi}{3\omega} \frac{di_d}{dt} \qquad 3.5.5$$

$$i_b = -i_d - \frac{\pi}{3\omega} \frac{di_d}{dt} \qquad 3.5.6$$

$$i_c = i_d + \frac{\pi}{3\omega} \frac{di_d}{dt} \qquad 3.5.7$$

So the rectified voltage in equation 3.5.4 can be given by:

$$V_d = \frac{3}{\pi} \int_{\frac{\pi}{3}+\alpha}^{\frac{2\pi}{3}+\alpha} \left\{ \sqrt{2}ECos\left(\theta - \frac{2\pi}{3}\right) - \sqrt{2}ECos\left(\theta + \frac{2\pi}{3}\right) \right\} d\theta - \frac{6l_c \omega \, i_d}{\pi} - 2l_c \frac{di_d}{dt}$$

After simplification dc voltage can be found as follows:

$$V_d = \frac{3\sqrt{3}}{\pi} ECos\,\alpha - \frac{6}{\pi}l_c\omega\,i_d - 2l_c\frac{di_d}{dt}$$ 3.5.8

Again applying KVL, the average dc current can be found by [27]:

$$V_d = R_{dc}i_d + L_{dc}\frac{di_d}{dt} + e_d$$ 3.5.9

The output dc current can be found by integrating above equation as follows:

$$i_d = \int \frac{\dfrac{3\sqrt{2}}{\pi}ECos\alpha - i_d\left(R_{dc} + \dfrac{6}{\pi}l_c\omega\right) - e_d}{L_{dc} + 2l_c}dt$$ 3.5.10

To get the q and d-axis components of the ac current, the dc current is assumed constant throughout the interval. The average-value of dc q- and d- axis currents is broken into two components of dc current (i_d) which are: commutation interval during which the current is transferred from T_1 to T_3 and the conduction interval during which T_2 and T_3 are conducting. So the current into the ac source must be in the form of following way:

$$i_{abc} = [i_a \qquad -i_d\,-i_a \qquad i_d]$$

And

$$V_{as} = V_{bs} = 0$$

$$\sqrt{2}ECos\theta + lc\frac{di_a}{dt} = \sqrt{2}ECos\left(\theta - \frac{2\pi}{3}\right)\theta + lc\frac{di_b}{dt}$$

After simplification current in phase can be found as [27]:

$$i_a = -i_d + \frac{1}{l\omega}\frac{\sqrt{3}}{2}\sqrt{2}E\left[Cos\alpha - Cos\left(\theta - \frac{\pi}{3}\right)\right]$$

57

The commutation subinterval ends when the current in T_1, which is the a-phase current becomes zero. The angle from the time T_3 is turned on & T_1 is turned off is known as the commutation angle u. So putting i_{ag} zero at the above equation, the commutation angle becomes [27]:

$$u = -\alpha + \arccos\left[\cos\alpha - \frac{l_c\omega\, i_d}{2}\right]$$

3.5.11

After commutation, the a-phase current remains at zero

$$i_{abc} = \begin{bmatrix} 0 & -i_d & i_d \end{bmatrix}$$

So here the average q and d-axis components can be established [34] as follows:

$$i_{q,com} = \frac{3}{\pi} \int_{\frac{\pi}{3}+\alpha}^{\frac{\pi}{3}+\alpha+u} i_{q,com}(\theta)d\theta$$

$$i_{q,cond} = \frac{3}{\pi} \int_{\frac{\pi}{3}+\alpha+u}^{\frac{2\pi}{3}+\alpha} i_{q,cond}(\theta)d\theta$$

$$i_{d,com} = \frac{3}{\pi} \int_{\frac{\pi}{3}+\alpha}^{\frac{\pi}{3}+\alpha+u} i_{d,com}(\theta)d\theta$$

$$i_{d,cond} = \frac{3}{\pi} \int_{\frac{\pi}{3}+\alpha+u}^{\frac{2\pi}{3}+\alpha} i_{q,cond}(\theta)d\theta$$

After simplification it is found that [27]:

$$i_{q,com} = \frac{2\sqrt{3}}{\pi} i_d \left[Sin\left(u + \alpha - \frac{5\pi}{6} \right) - Sin\left(\alpha - \frac{5\pi}{6} \right) \right] \frac{3}{\pi} \frac{\sqrt{2}E}{l_c \omega} Cos\alpha [Cos(u+\alpha) - Cos\alpha]$$

$$+ \frac{3}{4\pi} \frac{\sqrt{2}E}{l_c \omega} [Cos(2u) - Cos(2\alpha + 2u)] \qquad\qquad 3.5.12$$

$$i_{d,com} = \frac{2\sqrt{3}}{\pi} i_d \left[-Cos\left(u + \alpha - \frac{5\pi}{6} \right) + Cos\left(\alpha - \frac{5\pi}{6} \right) \right] \frac{3}{\pi} \frac{\sqrt{2}E}{l_c \omega} Cos\alpha [Sin(u+\alpha) - Sin\alpha]$$

$$+ \frac{3}{4\pi} \frac{\sqrt{2}E}{l_c \omega} [Sin(2u) - Sin(2\alpha + 2u)] - \frac{3}{2\pi} \frac{\sqrt{2}E}{l_c \omega} u \qquad\qquad 3.5.13$$

Similarly the conduction component can be found as:

$$i_{q,cond} = \frac{2\sqrt{3}}{\pi} i_d \left[Sin\left(\alpha + \frac{7\pi}{6} \right) - Sin\left(\alpha + u + \frac{5\pi}{6} \right) \right] \qquad\qquad 3.5.14$$

$$i_{d,cond} = \frac{2\sqrt{3}}{\pi} i_d \left[-Cos\left(\alpha + \frac{7\pi}{6} \right) + Cos\left(\alpha + u + \frac{5\pi}{6} \right) \right] \qquad\qquad 3.5.15$$

So the total d and q-axis current component can be calculated as

$$i_q = i_{q,com} + i_{q,cond} \qquad\qquad 3.5.16$$

$$i_d = i_{d,com} + i_{d,cond} \qquad\qquad 3.5.17$$

From the above equation 3.5.1 to 3.5.17 the required converter can be simulated with the help of SIMULINK. The subsystem representation is given in Appendix A.

3.6 Conclusion

In this chapter, MATLAB-SIMULINK is used to simulate the wind energy conversion system in the wind-diesel hybrid power system in Cartwright, Labrador and grid connected wind farm near St. Anthony. In Simulink different graphical blocks from built-in library can be used to connect together to simulate one equation. Several equations can be grouped together to form a sub-system. Linking all sub-systems together generate a full system. The sub-systems are given in Appendix A.

Chapter 4

Impact of a 250kW wind turbine on Cartwright diesel power system

4.1 Introduction

Cartwright is an isolated community in Southern Labrador, Canada. The community's main source of income is fishery. There is a crab plant operated by Labrador fisherman's union shrimp company, which is the community's main source of employment. A diesel plant is located in the community which is the main source of generation of electricity. The diesel plant is operated by Newfoundland Hydro. Four diesel generators with the total capacity of 2150kW are operating to supply electricity to the community [35]. The total diesel consumption by this diesel plant is about 1.2 million liters per year. Generation of electricity using diesel is costly for a small remote isolated

61

system. Figure 4.1 shows the location of Cartwright in Labrador. The nearest community, Battle Harbor is about 200km away from Cartwright.
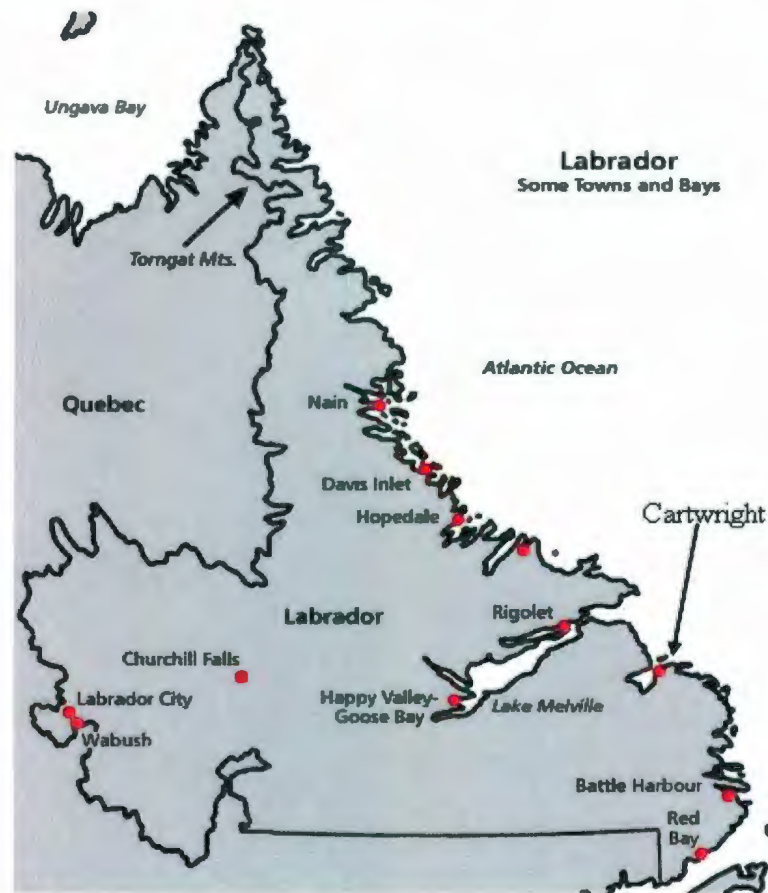
Figure 4.1: Location of Cartwright in Labrador

The most available renewable energy source in Cartwright is wind energy. Generation of electricity from wind is the fastest growing energy technology in the world. Wind-diesel system options are in exciting stage of exploration and development. A significant number of wind-diesel systems have been installed throughout the world to serve isolated remote load. For this community, wind turbine can be installed outside the community. At remote locations electricity generation from wind can help to reduce the overall operating costs by reducing the fuel costs. In this chapter the voltage and

frequency variation due to wind power addition to the existing isolated power system in Cartwright are determined.

4.2 Existing power system in Cartwright

Four diesel generators are installed in Cartwright to supply the electricity demand of the community which is shown in figure 4.2. A voltage level of 4.16kV is supplied to the community which is generated by two generators running at one time with line to line voltage of 600V. In this distribution layout only major loads are shown. A fish plant only operates during summer time. Most of the residents of this community heat up their houses by using wood or furnace oil.
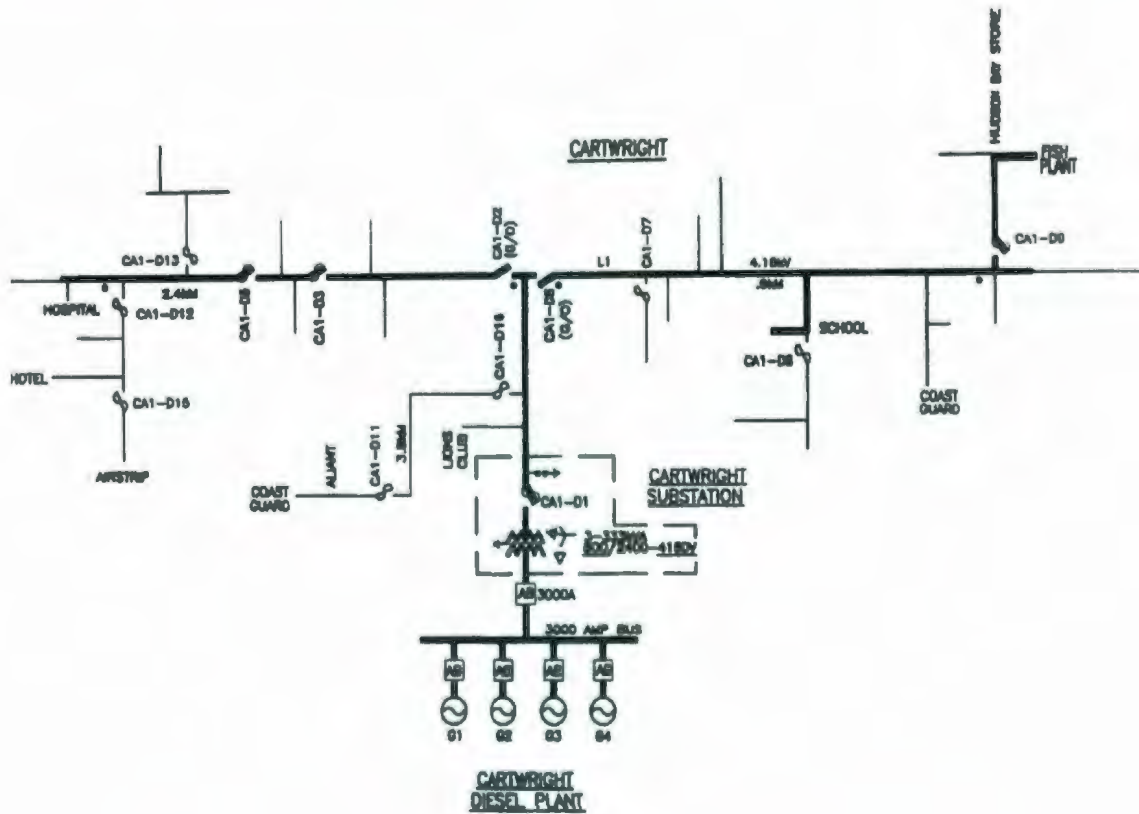
Figure 4.2: Existing power system in Cartwright
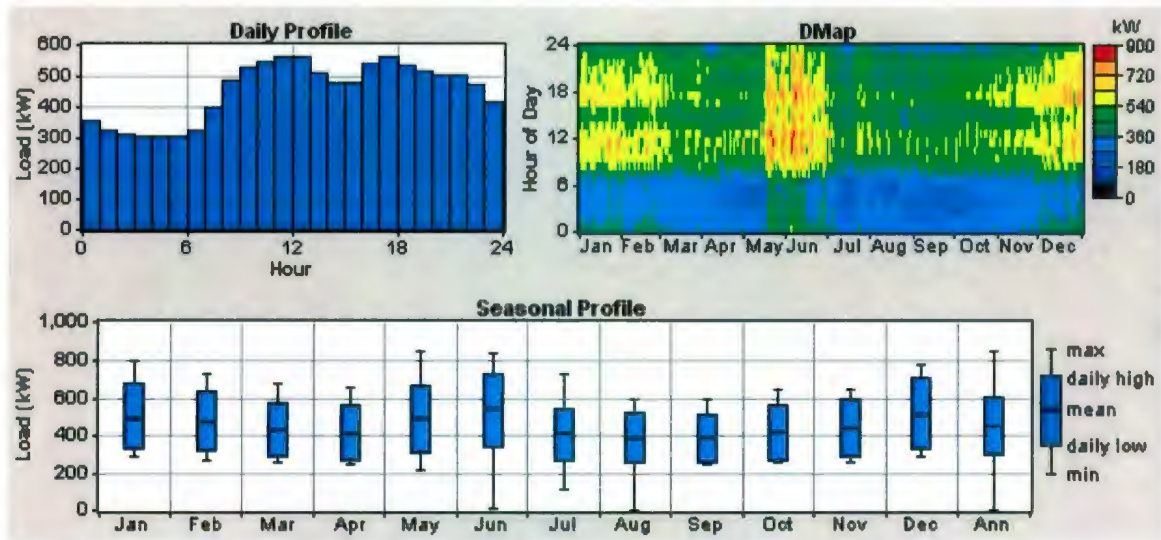
Figure 4.3: Load demand in Cartwright

From figure 4.3 it can be observed that the daily load profile varies from about 300kW to 550kW. From monthly load profile it is also noticeable that during summer, the load demand goes to its peak demand which is about 850kW. As the fish plant only operates during summer, most of the electricity demand is consumed by the fish plant during summer. DMap (data map) in the above figure shows one year of hourly data. With time of day on one axis and day of the year on the other, each hour of the year is represented by a rectangle which is colored according to the data value for that hour. The DMap allows daily and seasonal patterns to be seen much more easily than would be possible with a simple time series plot. The diesel plant has its own diesel storage tank which is maintained by a local oil supplier. The principal limitation of diesel power grid is the cost of power tends to increase as oil price is increasing day by day. Some other costs related to diesel plant such as the transportation cost, operation and maintenance cost also affect the cost of the electricity especially when the diesel plants are located in a remote isolated area.

4.3 Wind Energy Resources in Cartwright

To place a wind turbine in an area, it is important to discover the information about available wind energy resources for that particular area. Available wind resources or converted wind power can be used to select a wind turbine for that area. Environment Canada has a weather station near to the diesel plant in Cartwright. Yearly wind speed data can be found at [36]. Figure 4.4 shows the yearly data in Cartwright. The annual average wind speed is 5.02m/s at 10m anemometer height.
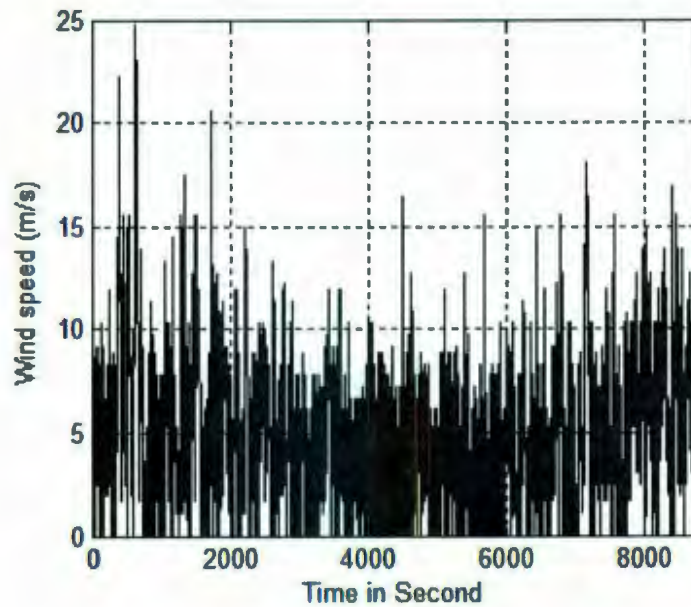
Figure 4.4: Annual wind data in Cartwright

Cartwright is situated on the southern cost of Labrador. The community's economy mainly based on fishery. Figure 4.5 shows the topographical location of Cartwright, Labrador. The scale of the map is 1:50000.

65

Figure 4.5: Topographical location of Cartwright

A 250kW wind turbine can be installed outside the community. To extract maximum power from wind, the turbine can be placed on top of any of the hill in the area. The small circles in figure 4.5 represent the top of the hills. To observe the voltage and frequency variation, different locations were considered to establish the wind turbine near to the community.

4.4 Dynamic simulation of Wind Diesel hybrid System

Figure 4.6 represents the complete wind-diesel hybrid power system of Cartwright. Block diagrams of the sub-systems are given in Appendix A. The values of the variables are given in Appendix B.

As the objective of this research work is to observe the voltage fluctuation and frequency variation by a 250kW wind turbine, only the wind speed parameter is considered for introducing voltage and frequency variation into the system. The voltage fluctuation and frequency variation were observed at the grid side and also at the wind turbine side. The bus voltage and frequency are determined by diesel system. Three phase

voltages are fed to wind turbine through transformer. The output currents from the wind turbine are fed back to the grid through a transformer. As wind speed is variable in nature so the current output from wind turbine will also vary according to wind speed. So the current variation from the wind turbine will also vary the voltage and current at the grid. The whole wind-diesel hybrid power system appeared to be difficult and slow. The model is solved with 'Variable Step/ode-45(Domand-Prince)' method. The relative and absolute tolerance was taken as $1e^{-3}$ and $1e^{-6}$ respectively.
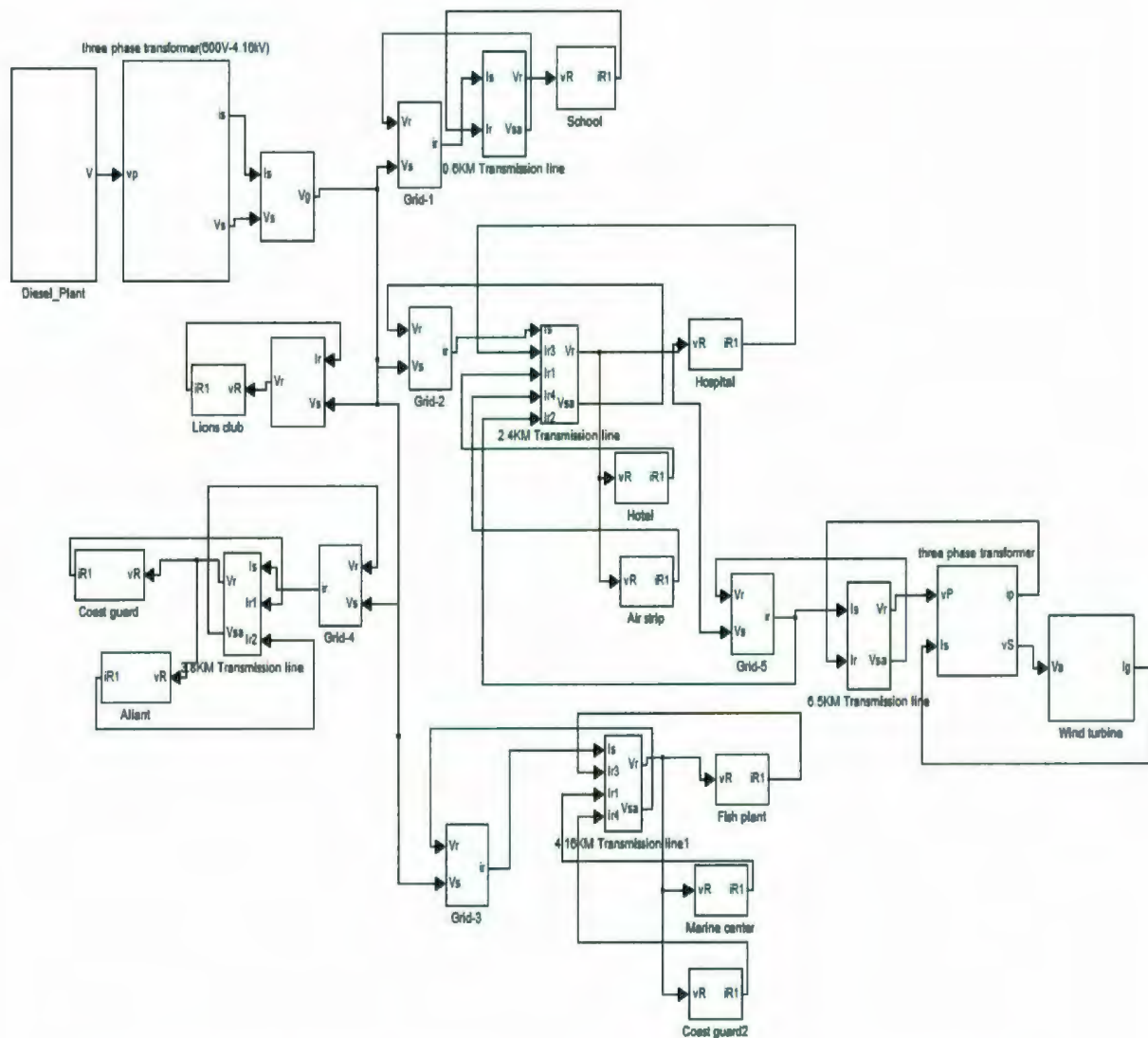
Figure 4.6: SIMULINK representation of Cartwright power system

During SIMULINK design the power system of Cartwright is divided according to the length of the transmission line mentioned in figure 4.2. Voltages are supplied to the load by the grid through a transmission line. The grid voltage is maintained by diesel plant through a step up transformer (diesel plant output is grid) A wind turbine is connected to the power system through a 13km transmission line. In an existing utility system driven by multiple diesel generators such as a remote location, the power quality required of a wind-diesel system will be determined by the utility itself. Wind turbine output is dependent on the nature of wind energy and diesel generator depends on the availability of diesel. The quality of power can be described by voltage stability, frequency variability, flicker, phase balance and power factor. The quality of power supplied by wind-diesel system in ideal condition should be purely sinusoidal voltage and constant frequency so that no fault should be developed within the components or consumer appliances. But in practice, voltage and frequency vary to some extent in an isolated system. The degree of deviation from its firm value can be used to measure the power quality. To reduce the degree of deviation, it is important to choose a good location for the wind turbine installation. Figure 4.7 shows the satellite image of a possible wind turbine location and distance from the diesel plant. From the figure it can be observed that a 250kW wind turbine can be installed on the top of a hill about 6.5km away from the community to extract maximum wind energy from the wind.
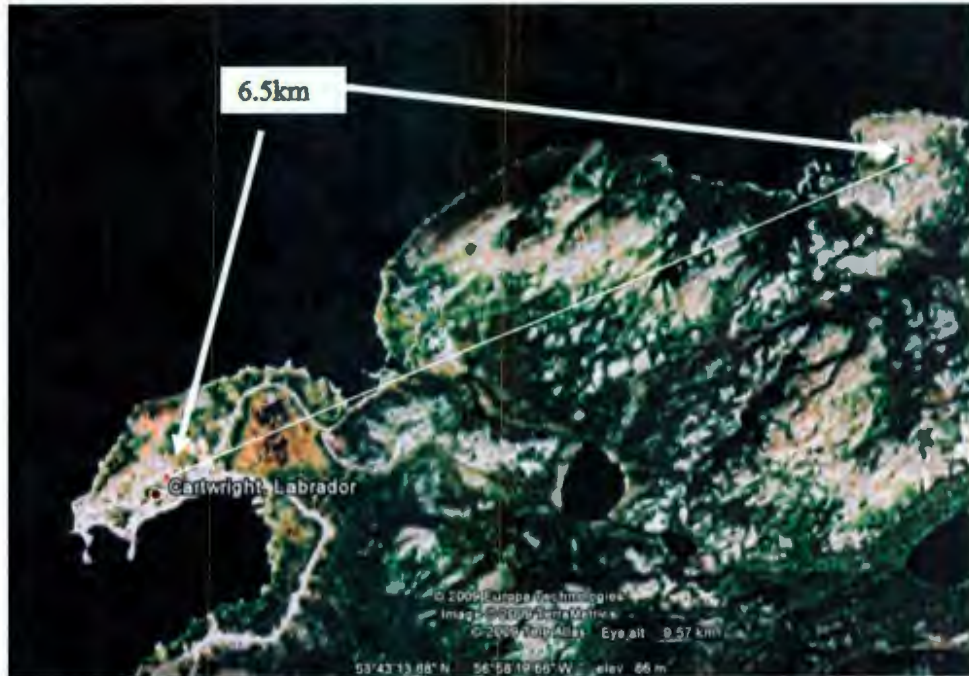
Figure 4.7: Wind turbine is placed 6.5km away from grid

To observe the voltage variation and frequency variation introduced by the wind turbine in Cartwright power system following wind speed data is used in the SIMULINK. Figure 4.8 shows the wind speed data for Cartwright over a 20sec time period.
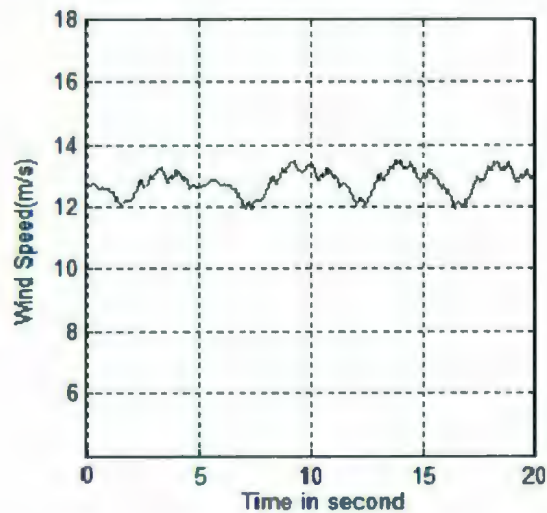

Figure 4.8: Wind Speed data in Cartwright

With the wind speed characteristics applied to the simulation, the wind turbine voltage, grid voltage and frequency variations are shown in figure 4.9 to 4.11 respectively.
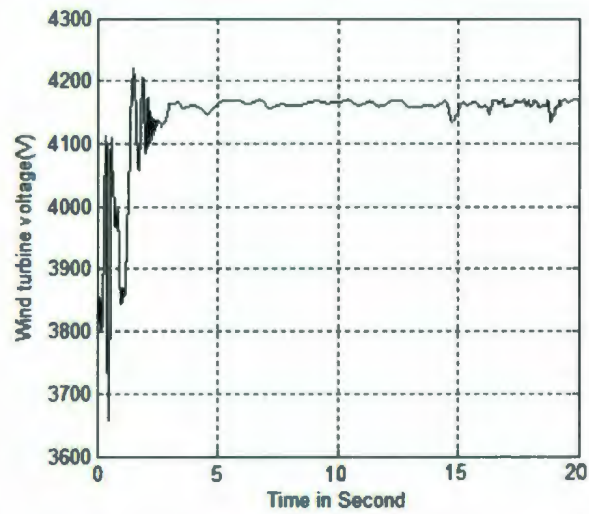
Figure 4.9: Variation of voltage at wind turbine

The variation of voltage at the wind turbine side is about 16.149V with the wind speed variation.
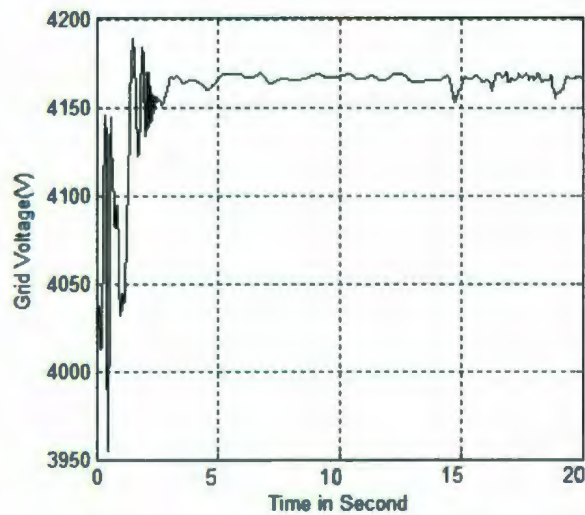
Figure 4.10: Variation of voltage at grid

70

The variation of voltage at the grid side is about 12.1784V due to the fluctuation of voltage generated by the wind turbine.
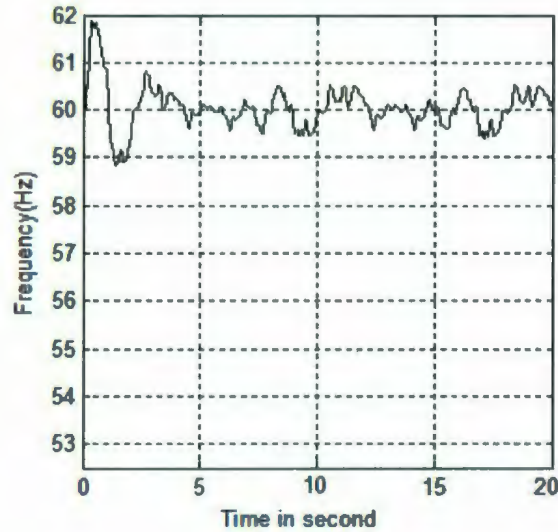

Figure 4.11: Variation of frequency

The frequency variation caused by the wind-diesel system is about 1.1Hz at the grid. As from figure 4.5 it can be seen that there are some hilly areas outside the community of Cartwright. So during simulation we have also observed the voltage fluctuations and frequency variation considering different placements of wind turbine from the grid. The simulation results are given in Table 4.1

Table 4.1 Voltage fluctuation and frequency variation for different length of transmission lines

Wind turbine distances (km)	Voltage fluctuation at grid (V)	Voltage fluctuation at wind turbine (V)	Frequency variation Hz
8	8.103	11.1	0.97
10	5.71	9.65	0.85
13	4.95	8.22	0.801

The above table shows that with increasing the distance of wind turbine from the grid can reduce the voltage fluctuation and frequency variation. The variation of voltage at the customer's terminals under any condition must be within the limit of $\pm10\%$ of the nominal voltage [15]. Frequency variation for large power system is allowed to vary within the range of <1%. Small wind-diesel hybrid power systems are allowed to operate within the variation of frequency is about $\pm3\%$ [15]. The above simulations show that voltage and frequency variations will be well in limits if a 250kW wind turbine is installed in Cartwright.

4.5 Conclusion

In this chapter the impact of a 250kW wind turbine on a remote isolated diesel power system is observed. From the above discussion it is found that a 250kW wind turbine can be installed outside of the community which can bring benefit to the community from the available wind energy in this area. As wind energy is variable in its nature, so to avoid sudden variation of voltage at the grid terminal and load end, the wind turbine can be placed at a suitable distance but it can't be placed far away from the diesel plant as attenuation characteristic of transmission line can reduce power flow to the grid. Voltage and frequency will be well in the limits after such an installation.

Chapter 5

Grid Impact of a 5.25MW Wind Farm near St. Anthony, Newfoundland

5.1 Introduction

St. Anthony is a town on the northern peninsula of Newfoundland. This region is connected to the Newfoundland island grid through a 248km transmission line and has one of the best wind resources in Canada. For remote locations, the powers supplied by diesel plants are associated with high fuel cost and high running cost. Power supply from central grid using long transmission lines is also associated with high maintenance cost, high protection cost and high transmission loss. This limitation of a remote area like St. Anthony can be reduced by proper uses of renewable sources available in that area. St. Anthony is situated in the northern side of Newfoundland, and is the largest of the

communities scattered along the great Northern Peninsula. It has a population of 2730 and is considered the service center for the most northerly communities on the island of Newfoundland. The economy is based mainly on three sectors, namely the fishery, institutions and retail/service industries. Until recently a 6000kW diesel generating plant was used to supply power to the town. The plant is now used for emergency purposes. Now the electrical power is delivered from the Newfoundland central grid through a 248km transmission line.

St. Anthony is located in one of the wind abundant areas of the province. Annual average wind speed recorded is about 7.1m/s, which is one of the highest wind power regions in Canada. Wind farm development can be divided into a number of phases such as initial site selection, project feasibility assessment, construction and operation. An initial assessment of various sites and the selection of a suitable site were under taken several years ago [37]. A summary of the assessment given in the Appendix C. The size of the selected location is determined using the sizing tool called HOMER [38]. After determining the size of the wind farm the dynamic modeling and simulation of the wind farm were carried out to determine the voltage and frequency variation. Details of the study are provided below.

5.2 SIZING OF WIND FARM:

The initial site assessment is given in Appendix C resulted in Cape Norman being identified as one of the best sites in that region to establish a wind farm. The inputs to HOMER are wind speed data, load data, wind turbine characteristic curve,

74

turbine costs and system constraints. Environment Canada has a weather station at St. Anthony airport. The annual wind data for St. Anthony is shown in Figure 5.1 [36].
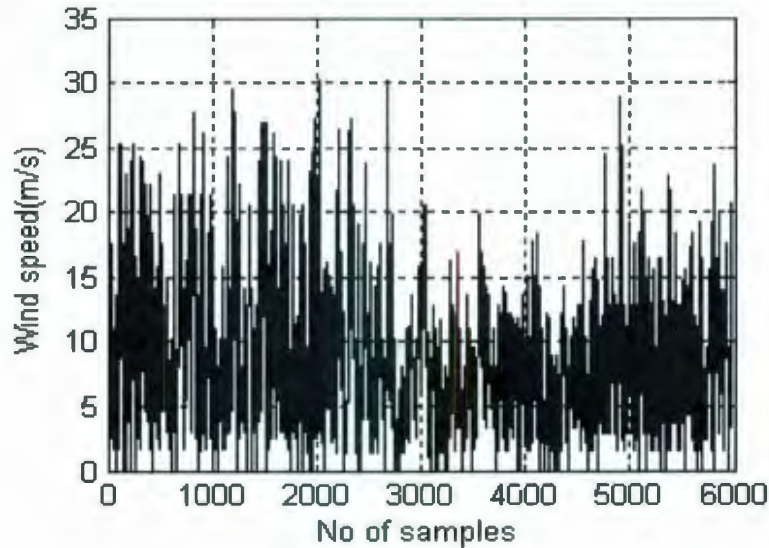

Figure 5.1: Annual wind data in St. Anthony

From the wind speed data it is found that the average wind speed is about 8.85m/s at 32.9m height, which is one of the highest wind resource regions in Canada. The wind speed data was only available for St. Anthony, so the one year wind data for Cape Norman was obtained by scaling the St. Anthony wind data using the average values [39]. The seasonal mean wind speed value for Cape Norman is given in Table 5.1.

Table 5.1: Average wind data in Cape Norman

Period	Months	Mean Wind Speed
Winter	December/January/February (DJF)	11.81 m/s
Spring	March/April/May (MAM)	9.83 m/s
Summer	June/July/August(JJA)	7.15 m/s
Fall	September/October/November(SON)	9.12 m/s
Annual		9.46 m/s

The annual average wind speed for Cape Norman is 9.46m/s at 30m elevation. Scaled data for Cape Norman is shown in Figure 5.2. From the wind speed data it can be seen that the maximum and minimum power production from the wind farm can be expected during winter and summer respectively. Figure 5.2 indicates that there is a significant wind resource to develop a wind farm, which in association with the grid can supply the power required for the St. Anthony area.
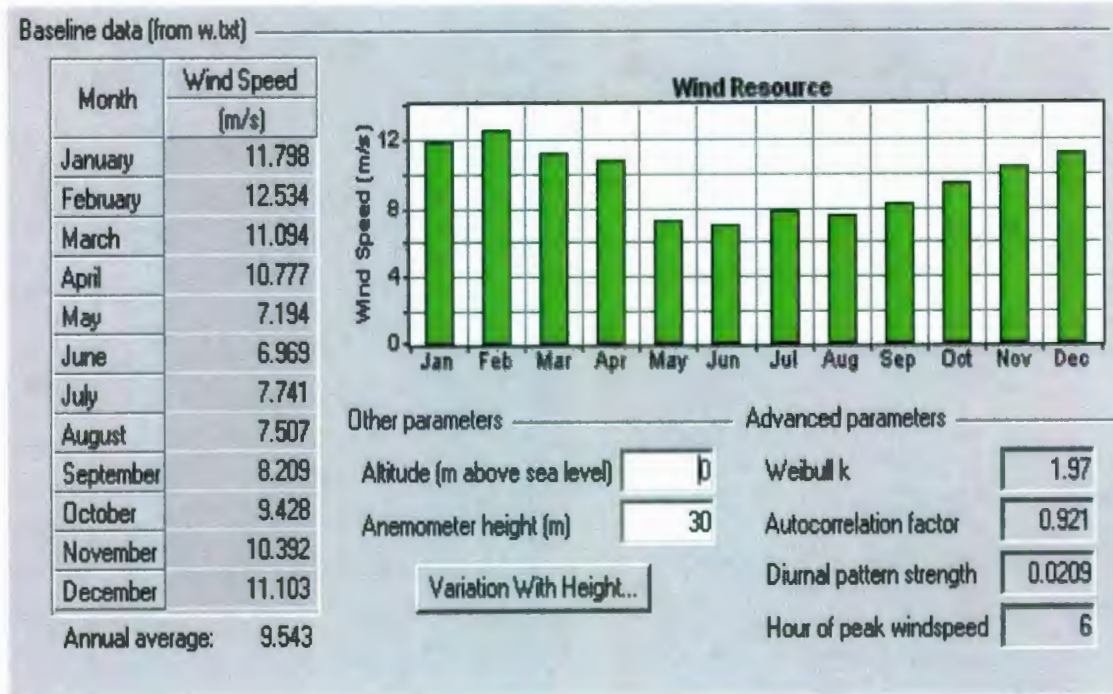

Figure 5.2: Cape Norman scaled annual wind speed data

The load data for St. Anthony region was collected from Newfoundland Hydro which is shown in Figure 5.3.
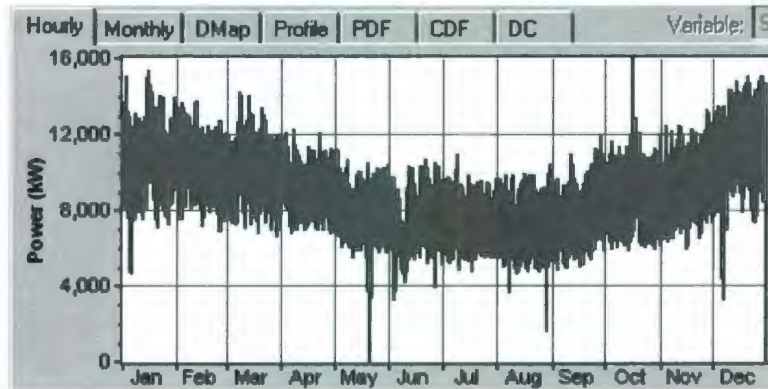
Figure 5.3: Annual load data for St Anthony region

From the load data it is found that the average load demands is higher in fall and winter season and less in the summer and spring season. The 250kW sized induction generator type wind turbines were used for the sizing tool. The cut in speed of the wind turbine is about 3m/s and the rated speed is about 12m/s. The proposed hybrid power system designed for St. Anthony is shown in Figure 5.5. Sizing of the hybrid power system can be done using HOMER, assuming a constant load in near future. Different sizes of wind turbine can be used for constructing a wind farm. In practice, the price of a wind turbine decreases with the increasing size of the wind turbine. But the large sized wind turbine can't be selected as the site is remotely located which can increase the transportation cost and installation cost. Another issue is unavailability of a large crane in Newfoundland. Mid sized 250kW wind turbine was selected for the wind farm considering price, installation and maintenance issues. Price for wind turbine was obtained from its manufacturer.

77

Figure 5.4: Satellite image of St Anthony and Cape Norman
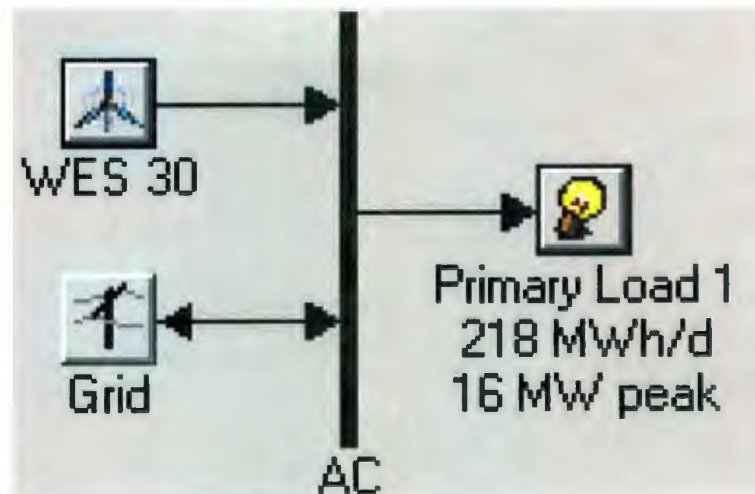
Figure 5.5: Proposed hybrid power system

The satellite image in Figure 5.4 shows that the proposed wind farm site is almost 50 km away from the locality of St. Anthony. In the HOMER simulation it is assumed that the interest rate is 8% and the project life time is 25years. The amount of wind generation that can be integrated into the current island grid system is limited to approximately 80 MW [40]. Currently 54 MW wind generation is installed in the province and another still 26 MW wind generation can be integrated into the power grid

of Newfoundland. A 5.25MW wind power addition would lead to a renewable energy fraction of about 30% in St. Anthony region. With a condition of about 30% renewable energy fraction, the optimized homer simulation results are shown in Figure 5.6.

	WES30	Grid (kW)	Initial Capital	Operating Cost [$/yr]	Total NPC	COE [$/kWh]	Ren. Frac.
	21	14400	$14,332,499	6,081,211	$79,248,056	0.093	0.27
	20	14400	$13,649,999	6,169,798	$79,511,208	0.094	0.26
	19	14400	$12,967,500	6,258,384	$79,774,344	0.094	0.24
	17	14400	$11,602,500	6,435,557	$80,300,632	0.095	0.22
	15	14400	$10,237,500	6,612,725	$80,826,856	0.095	0.19
	14	14400	$9,555,000	6,701,311	$81,090,000	0.096	0.18

Figure 5.6: HOMER optimized result

Figure 5.6 shows that the hybrid power system will need 21, WES30 (induction generator type) 250kW wind turbines along with 14400kW electricity demand from the grid with excess electricity almost 0.0%. Twenty one wind turbines were selected to keep renewable energy fraction below 30% as the maximum possible renewable energy addition to Newfoundland grid is 80MW. Initial cost for this system will be approximately $14,332,499 with a production cost of electricity at $0.093/kWh. The expected electrical performance of the hybrid power system is shown in Figure 5.7.
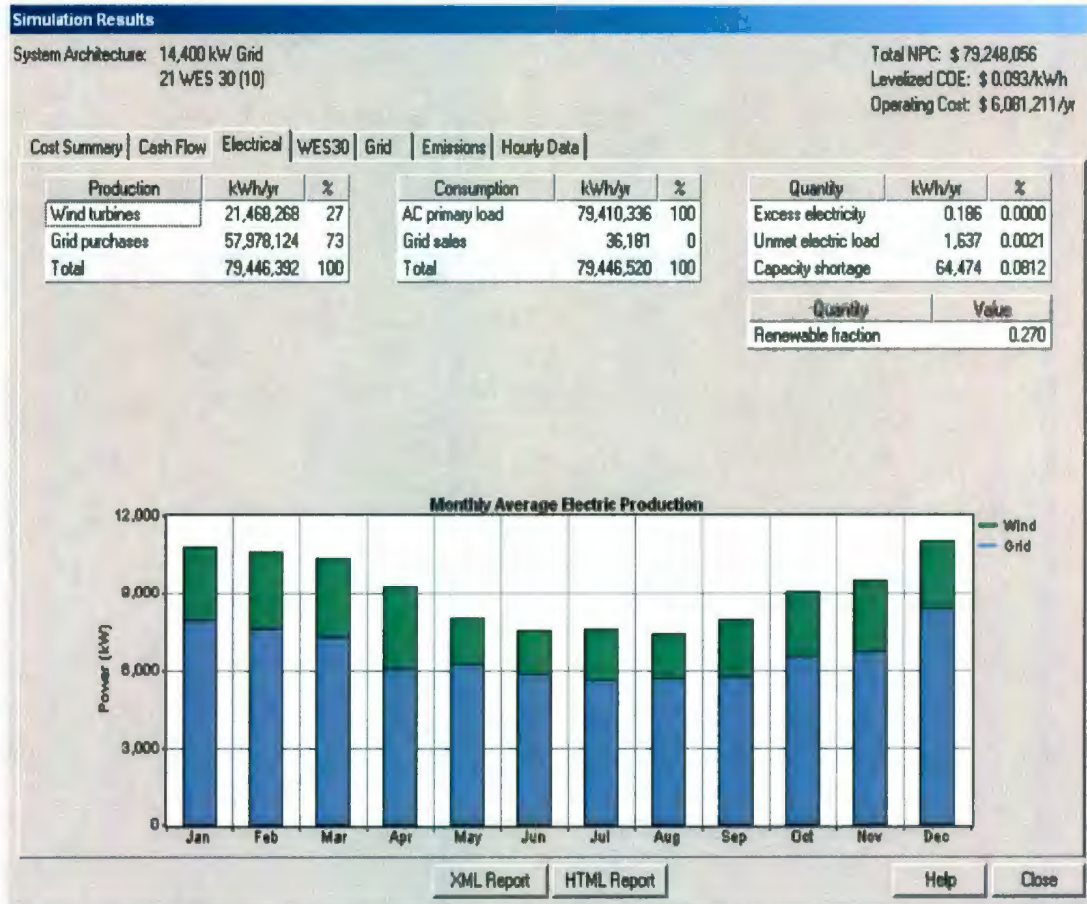
Figure 5.7: Electrical performance of the proposed hybrid power system

Figure 5.7 shows that more electricity will be produced from the wind farm during the winter season and less energy will be produced during the summer season. Figure 5.7 also shows that the total electrical energy required for that area is 79,446,392kWh/year of which 73% will be met by the grid including the system peak demand. The rest of the electricity, which is about 21,468,268kWh/yr, will be met by the installed 5.25MW wind farm with a renewable fraction of 27%. From Figure 5.7 it can be seen that the excess of electricity in the hybrid power system of St. Anthony area is almost 0.0% and unmet electric load is also about 0.0%.

In order to determine the annual energy output from the wind farm it is required to know the annual energy output from each wind turbine in the wind farm. The annual

energy output of a turbine can be obtained from the capacity factor of the wind turbine throughout the year and the capacity or use factor is obtained using the following formula.

$$\text{Use factor} = \frac{\text{Actual amount of power produced over a time}}{\text{Power could be produced if turbine operated at maximum output 100\% of the time}}$$

The results of the calculation above are shown in Table 5.2, which indicate that the maximum energy output from a wind turbine is about 240.42MWh with use factor of 43.91% during the winter time of the year.

Table 5.2: Wind turbine output for annual and different times of the year

Period	Months	Power output	Energy output	Capacity factor
Winter	December/January/February (DJF)	109.77KW	240.42MWh/period	43.91%
Spring	March/April/May (MAM)	87.43KW	191.48MWh/period	34.97%
Summer	June/July/August(JJA)	61.65KW	135.03MWh/period	24.66%
Fall	September/October/November(SON)	69.7KW	152.66MWh/period	27.88%
Annual		80.97KW	709.36MWh/year	32.39%

From Table 5.2 it is observed that the annual energy output from a wind turbine at Cape Norman will be 709.36MWh/yr. The HOMER optimization results show that a 5.25MW wind farm can be installed at Cape Norman to supply electricity to St. Anthony and local area.

5.3 Dynamic simulation of grid connected wind farm

Numerous technical issues arise during the construction and integration of a wind farm. One of the common issues is what should be the placement of wind turbines in a wind farm. The available wind resource can vary within the wind farm. Wind turbines that are upwind of other wind turbines may cause lower wind speeds at the downwind turbines and increased turbulence. Consequently, the wind farm will not produce 100% of the energy that a similar number of isolated turbines would produce in the same prevailing wind. Energy loss within the wind farm can be reduced by optimizing the location of wind turbines within the wind farm. Assuming conservation of momentum the equation for the velocity deficit at a distance x, downstream can be given by [41].

$$U_x = U_o \times \left\{ 1 - \frac{1 - \sqrt{1 - C_T}}{\left(1 + 2K\dfrac{x}{D} \right)^2} \right\} \qquad 5.3.1$$

With the help of the above equation the wind turbines within the wind farm are placed in such way that the wind speed loss within the wind farm is minimized. Here C_T is the turbine thrust co-efficient, K is the wake decay constant which is 0.075 for upstream turbine and 0.11 for downstream turbine; X is distance measured between turbines, D is rotor diameter, and U_o is initial free stream velocity. The above equation can be used to decide the distances among wind turbines within a wind farm to keep array loss within 5%.

Another technical issue arises during the integration of wind farm with the grid. Wind farm operation results in fluctuating real and reactive power levels and may result

in voltage and current transients. Wind turbines, especially fixed speed turbines connected to the electrical grid, generally use induction generators which provide real power to the system and absorb reactive power from the system. Changes in the mean power production and reactive power needs of a wind farm can cause steady state voltage and frequency change in the connected grid system. The changes occur over numerous seconds. The weaker the grid, the greater the voltage fluctuations. In this section the variation of voltage and frequency at St. Anthony local load side through out the year due to the installation of wind farm at Cape Norman is investigated.

The distance between St. Anthony locality and Cape Norman along the road is almost 50km. A 50km transmission line is therefore assumed between the grid and the wind farm. At present the locality is being supplied by a central 138kV grid through a 248km transmission line. The proposed grid connected hybrid power system is shown in Figure 5.8 which shows a 138kV grid connected to the average load of St. Anthony (which is about 8.55MW) through a 248km transmission line and a 138/25kV transformer. A pi-model is used to represent the transmission line. The voltage produced at the wind farm is stepped up to 25kV to supply the local load through a 50km distributed transmission line.

Within the wind farm sub-system there are twenty one 250kW wind turbines connected together to the grid through 480V/25KV step-up transformer. In this simulation variable wind speed is applied to wind turbines within the wind farm. So the output from the wind turbines will also vary according to the wind speed. This variation of voltage and current will travel through the 50km transmission line to the grid side causing voltage and frequency variation at the load. This model is solved with variable

step/ode45 (Dormand-Prince) method. The absolute and relative tolerances are assumed to be 1e^{-5} and 1e^{-3} respectively.
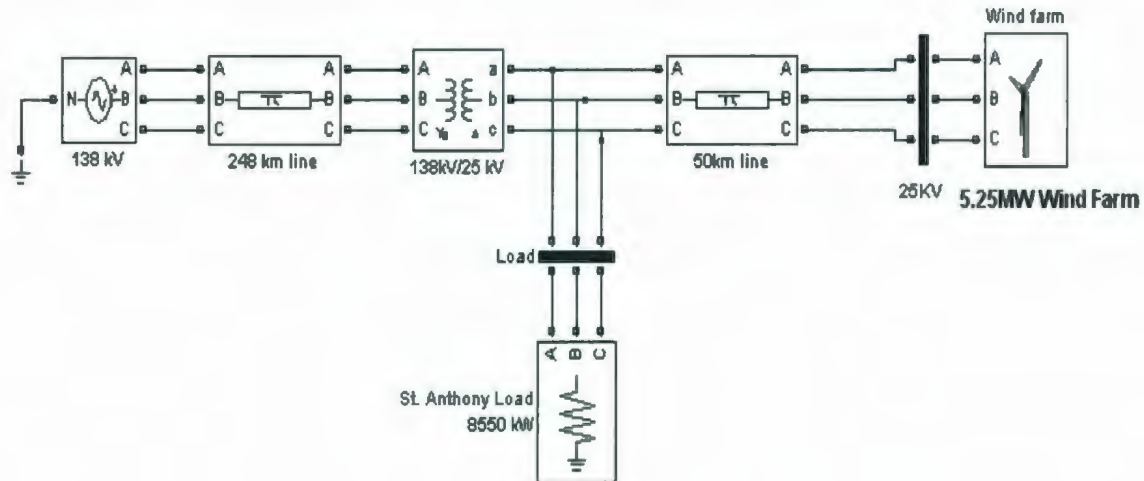
Figure 5.8: Proposed grid connected wind farm in St. Anthony

In order to observe the voltage and frequency variation the year is divided into four seasons. To observe the voltage variation and frequency variation in winter, the scaled winter wind speed data for Cape Norman is used in the SIMULINK Simpower blockset. Figure 5.9 shows the scaled winter wind speed data for Cape Norman over a 20sec time period.
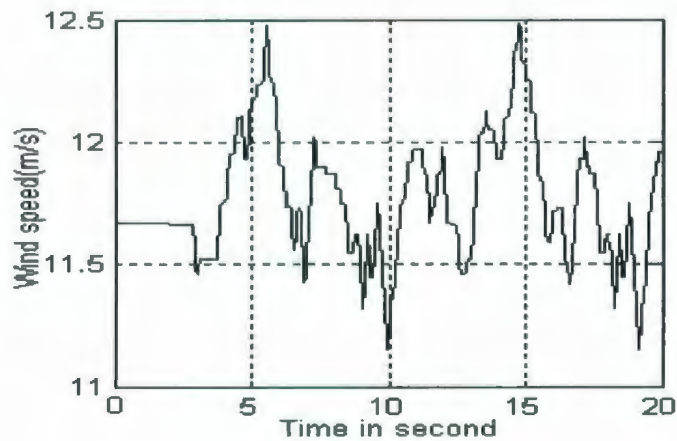
Figure 5.9: Scaled winter wind speed data for Cape Norman

With the wind speed characteristics applied to the simulation, assuming a constant load of 8550kW at St. Anthony, the expected load voltage variation is shown in figure 5.10 and expected frequency variations are shown in Figure 5.11.
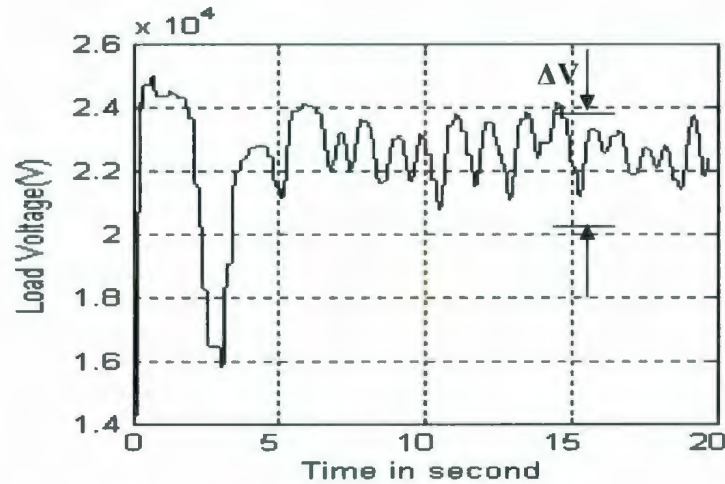
Figure 5.10: Load Voltage variation
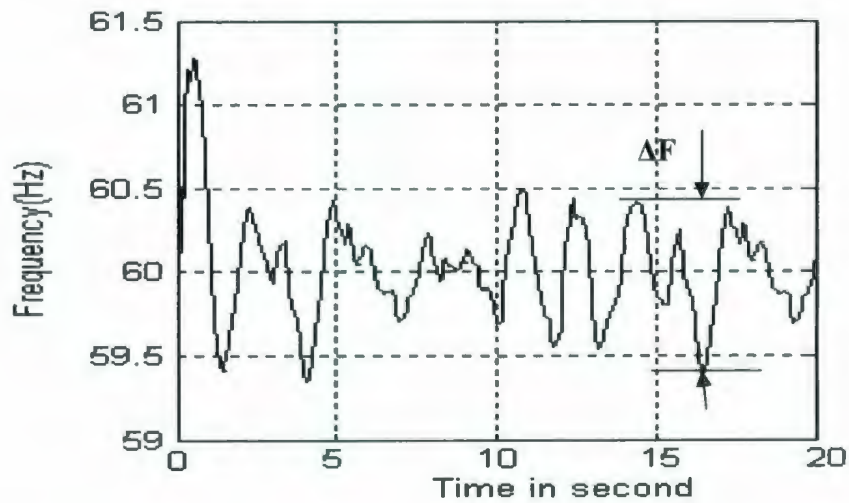
Figure 5.11: Load frequency variation

From Figure 5.10 it can be seen that during winter (DJF) the expected voltage variation is about 1975V (i.e.7.9%) and from figure 5.11 for the same wind speed the

frequency variation is about 0.942Hz. According to power quality standard EN50160, the voltage variation at the customer sides are required to be within $\pm10\%$ [42]. The voltage variation can be counteracted by adjusting the power factor of the wind turbines [43]. It has been observed that at nights with low system loads and high wind speeds, the wind farms can provide up to 75% of the total system load without problems [44]. Following the procedure outlined above, the results of the load and frequency variations for other seasons are shown in table 5.3.

Table 5.3: Voltage and frequency variation in St. Anthony due to 5.25MW wind farm

| Period	Voltage Variation	Frequency Variation
Spring(MAM)	1860V (7.48%)	0.789Hz
Summer(JJA)	1620V (6.5%)	0.652Hz
Fall(SON)	1570V (6.28%)	0.608Hz

From Table 5.3 it can be seen that the least variation of voltage and frequency occurs during the fall (SON). It can be seen that the voltage variation in St Anthony through out the year is within the tolerable voltage limit specified by EN50160 standard.

5.4 Conclusion

It is well known that wind is a highly unstable resource. Substantial changes are found on time scales of less than a few hours. To fully benefit from a large fraction of wind energy in an electrical grid, it is necessary to know in advance the electricity production generated by the wind farm. In this chapter the size of a wind farm for St. Anthony based on the one-year wind speed data and load data has been determined. It is

found that a wind farm consisting of twenty one, 250 kW wind turbine is adequate to provide up to 27% of the load in St. Anthony region. During winter the maximum voltage variation will be about 7.9% and a minimum variation will occur during the fall, which is about 6.28%. So due to wind energy addition to the St Anthony local grid, it is found that the variation of voltage throughout the year is within the limit of $\pm$ 10% specified by power quality standard EN 50160. So based on above evaluation it is suggested that a 5.25MW wind farm can be installed in Cape Norman for the area of St. Anthony.

Chapter 6

Conclusions and Recommendations

6.1 Introduction

At present in Canada the installed wind energy capacity accounts only for 1% of total electricity demand but the Canadian Wind Energy Association anticipates to increase the number to at least 20% by 2015 [45]. So extensive research and project developments are going on to explore more wind energy throughout the country to meet the electricity demand. Most of the new installations in Canada are grid connected. More than 300 remote communities in Northern Canada are far from the existing utility grid power system. These communities are the significant opportunities for the researchers to do their researches on wind energy addition in Canada. Frequently, diesel-powered generators are used to provide electrical power to remote isolated communities, often at substantial cost. Power supply from central grid using long transmission lines has very high maintenance cost, high protection cost and high transmission loss. Diesel powered

electrical system also have high maintenance cost and operational costs to the local isolated community due to the high fuel cost and transportation cost. Using on-site renewable energy such as wind energy and small hydro in addition to diesel generators reduces overall electricity generation costs and leads to safe and clean environment for the future generations.

6.2 Conclusions of research

In this research two remote communities in the province of Newfoundland and Labrador are selected to study the opportunity for the exploration of wind energy. In both cases voltage fluctuation and frequency variations which can be caused by the addition of wind energy were studied based on available wind speed and load data.

To investigate the validity of any proposed isolated wind-diesel hybrid power system, it is important to get the information about the present wind energy and also the impact of wind energy on existing diesel power system. To study the impact of wind energy on diesel driven power system in Cartwright, mathematical models for all different system components are developed and used to simulate the system in SIMULINK. In chapter 4 the impact of a 250kW wind turbine on Cartwright diesel power system is observed. It is found that a 250kW wind turbine can be installed outside the community. The tentative voltage fluctuation and frequency variation caused by the addition of wind energy to the existing diesel power system is within limit described by other researchers. In that chapter it is also found that as wind energy is variable in its nature, so to avoid sudden variation of voltage at the grid terminal and load end, wind turbine can be placed at a suitable distance but it can't be placed far away from the grid

as attenuation characteristic of transmission line can reduce power flow to the grid. So chapter 4 provides the details opportunity for the installation of a 250kW wind turbine in Cartwright, Labrador.

In chapter 5 a detailed study was carried to establish a wind farm near St. Anthony, Newfoundland. To establish a wind farm it is also important to consider environmental impact on the community. In this research it is found that to establish a 5.25MW wind farm for the area of St. Anthony, Cape Norman is the best location for the wind farm. A complete sizing of wind farm is carried out in HOMER based on available wind resource and load profile for the area. It is found that a 5.25MW wind farm can be installed based on twenty one 250kW wind turbine in Cape Norman to supply electricity demand in St. Anthony. Dynamic simulation is carried out to observe the voltage fluctuation and frequency variation in St. Anthony area through out a year due to the addition of wind farm in Cape Norman. From Dynamic simulation it is found that the maximum voltage variation will be of about 7.9% will occur during winter and a minimum variation will occur during the fall, which is about 6.28%. Here it is found that the variation of voltage throughout the year is within the limit of $\pm$ 10% specified by power quality standard EN 50160. So from chapter 5 it is suggested that a 5.25MW wind farm can be installed in Cape Norman for the area of St. Anthony.

6.3 Recommendations for improvement

Future work can be done to study the power quality in wind-diesel or grid connected wind farm. For wind-diesel system the following recommendations are suggested.

- Based on available site information both types of wind turbine i.e. variable speed and fixed speed can be considered. In this study only fixed speed wind turbines were considered. In future work modeling of variable speed wind turbines and its power electronics can be done and it is highly recommended.

- Study of variable speed wind turbine power electronics generated harmonics on an isolated wind-diesel grid is also recommended.

- Different types of long term and short term storage systems can be used with the proposed wind-diesel system to store excess electricity at minimum load.

- Dump load can be incorporated into the wind-diesel system to dissipate excess energy produced by wind turbine which can no be stored.

- The standard controllers for the individual system can be utilized based on minimum diesel run, dumping excess energy, filtering wind power. Therefore, a detailed study of dynamic controller as well as supervisory controller is also suggested.

For grid connected wind farm the following recommendations are suggested.

- Variable speed wind turbine with voltage controller can be used to reduce voltage variation.

- To reduce transmission loss HVDC system can be used to transmit power from wind farm to local power grid.

- Soft starters can be used to integrate wind farm with the power grid so that less voltage fluctuation results during switching of wind turbines within the wind farm. No soft-starter were modeled or studied in this work.

- The wind turbines equipped with controllable source of reactive power such as SVC or STATCON can be used to deliver reactive power required to increase the speed so that steady voltage are maintained.

- It is also suggested to use some fast computing facility like Atlantic Computational Excellence network (ACE net) to simulate the system for a long duration wind data. In this study only personal computers were used and the simulation time was limited to only 20 Seconds. One simulation took few days to process only 20 Seconds wind data.

References:

1. www.wwindea.org.

2. www.canwea.ca.

3. J.F. Manwell, J.G. McGowan and A.L. Rogers, "Wind Energy Explained- theory, Design and Application" John Wiley & Sons Ltd, 2002.

4. Sharpe, L. "Offshore generation looks set to take off", IEE Review, Volume: 48 Issue: 3, pp. 24 –25, May 2002.

5. Grainger, B.; Thorogood, T., "Beyond the harbour wall", IEE Review, Volume: 47 Issue: 2, pp. 13 –17, March 2001.

6. Tande JOG., "Grid integration of wind farms", Wind Energy, Volume: 6; pp. 281 – 295, 2003.

7. Tande JOG., Jørgersen P, "Wind turbines impact of voltage quality". Preceding of EWEA '96, pp. 3 -8, 1996.

8. Tande JOG., Uhlen K., "Wind Turbine in Weak Grids – Constraints and Solutions" CIRED2001, 18-21 June 2001, Conference Publication No. 482, pp. 5, IEE 2001.

9. Chen Z., "Issues of connecting wind farms into power systems" 2005 IEEE/PES Transmission and Distribution Conference & Exhibition: Asia and Pacific Dalian, China, pp. 6, 2005.

10. Chuong T.T., "Voltage stability investigation of grid connected wind farm", Proceedings of World Academy of Science, Engineering and Technology, Volume 32, ISSN 2070-3740, pp. 42-48, August, 2008.

11. Chen Z. and Spooner E., "Grid Power Quality with Variable Speed Wind Turbines" IEEE Transactions on Energy Conversion, Volume 16, No. 2, pp. 148 – 154, June 2001.

12. Muyeen S.M. and Shishido S., "Application of Energy Capacitor System to Wind Power Generation", Wind Energy, Volume 11, pp. 335-350, July/August 2008.

13. Bialasiewicz J.T. and Muljiadi E., "The Wind Farm Aggregation Impact on Power Quality" ECON Proceedings (Industrial Electronics Conference), IECON 2006 - 32nd Annual Conference on IEEE Industrial Electronics, pp.: 4195-4200, 2006.

14. Feltes C. and Erlich I., "Variable Frequency operation of DFIG based wind farms connected to the grid through VSC-HVDC link", Power Engineering Society General Meeting, 2007. IEEE 24-28, pp.:1 – 7, June 2007.

15. Hunter R. and Elliot G., "Wind – Diesel System, A guide to the technology and its implementation", Cambridge University Press, Cambridge, UK, 1994.

16. Tsitsovits A.J., Freris L.L., "Dynamics of an isolated power system supplied from diesel and wind" Volume 130, pp.: 587-595, 1983, ISSN: 0143-702X.

17. Jindal A.K., Gole A.M. and Muthumuni D., "Modeling and Performance Analysis of an Integrated Wind/Diesel Power System for Off-Grid Locations", Fifteenth National Power System Conference, IIT Bombay, pp.: 574 – 579, December 2008.

18. Hee S. K., Jatskevich J., "Power quality control of wind-hybrid power generation system using fuzzy-LQR controller", Energy Conversion, IEEE transaction, Volume 22, pp.: 516-527, 2007.

19. Iglesias I.J., Garcia L., Agudo A., Cruz I. and Arribus L., "Design and Simulation of a Stand alone wind diesel generator with a fly wheel energy storage system to supply the required active and reactive power." Power Electronics Specialists Conference, Galway, Ireland, Volume 3, pp.: 1381 – 1386, 2000.

20. Fadaeienedjad R., Moschopoulos G. and Moallem M., "Flicker Contribution of a wind turbine in a stand-alone Wind-Diesel system", CCECE/CCGEI, Niagara Falls. Canada, pp.: 233 – 238, May 5-7 2008.

21. Choi S.S. and Larkin R., "Performance of an autonomous diesel-wind power system", Electric Power Research, Volume 33, Issue 2, pp.: 87-89, May 1995.

22. Ackermann T., "Wind Power in Power Systems", John Wiley & Sons Ltd, 2005.

23. Siegfried Heier, "Wind Energy Conversion System", John Wiley & Sons ltd, 2006.

24. K. Rajambal and C. Chellamuthu, "Modelling and Simulation of Grid Connected Wind Electric Generating System," IEEE Trans on Energy Conversion, vol. 3, pp. 1847- 1852, Oct. 2002.

25. Blaabjerg F., Sørensen P., Hansen A.D., Lov F., "Wind Turbine Blockset in Matlab/Simulink-General Overview and Discription of Model" ISBN 87-89179-46-3, Institute of Energy Technology, Aalborg University.

26. Ozpineci, B., Tolbert, L.M., "Simulink implementation of induction machine model - a modular approach", Electric Machines and Drives Conference, 2003. IEMDC'03. IEEE International, Volume: 2, pp. 728 – 734, 1-4 June, 2003.

27. Krause, P.C., Wasynczuk, O. and Sudhoff, S.D."Analysis of Electric Machinery", IEEE Press, 2002.

28. Ong,Chee-Mun, "Dynamic Simulation of Electric Machinery: Using Matlab/Simulink", Prentice Hall PTR, 1997.

29. J. Duncan Glover, Mulukutla S. Sarma, "Power System Analysis and Design" 3rd Edition, Pws Pub Co., 2001.

30. Stevenson W.D., "Elements of Power System Analysis", McGraw-Hill, International Edition 1996.

31. Fitzgerald A.E., Kingsley C., and Umans S.D., "Electric Machinery" 6th Edition, McGraw Hill, 2003.

32. Ramtharan G. and Jenkins N., "Modelling and control of Synchronous Generators for Wide range Variable Speed Wind Turbines." Wind Energy Journal, 2007, Volume 10, Pages: 231-246.

33. Rashid Muhammad H., "Power Electronic Handbook" Academic press, 2001.

34. Sundhoff S.D., Corzine K.A., Hegner H.J. and Delisle D.E., "Transient and Dynamic Average Value modeling of Synchronous Machine Fed Load-Commutated Converters", IEEE Transactions on Energy Conversion, Vol.11, No.3, pp.: 508-514, September 1996.

35. Iqbal T., "Sizing of a wind-diesel hybrid power system for Cartwright Labrador", World Wind Energy Conference, June 24-26, Kingston, Ontario, Canada, 2008.

36. www.climate.weatheroffice.ec.gc.ca/climateData/canada_e.html.

37. Remote Community demonstration Program of Energy, Mines and Resources Canada, "Assessment of wind energy potential, St Anthony, Newfoundland", March 1985, prepared by Fenco Newfoundland Limited, St. Johns, Newfoundland.

38. www.nrel.gov/homer.

39. www.windatlas.ca.

40. www.nlh.nl.ca.

41. Manwell J.F., McGowan J.G. and Rogers A.L., "Wind Energy Explained- theory, Design and Application" John Wiley & Sons Ltd, England, 2002.

42. Voltage Characteristics of Electricity Supplied by Public Distribution Systems. EN-50160, 1995.

43. Tande JOG., SINTEF Energy Research, N-7465 Throndheim, Norway "Grid Integration of Wind farms", WIND ENERGY. Volume 6, pp.: 281 – 295, 2003.

44. Ackermann Thomas and Soder Lennart "Wind Energy Technology and Current Status: a review", Renewable and Sustainable Energy reviews, Volume 4, pp.: 315-374, 2000.

45. www.canadiangeographic.ca.

Appendix A

MATLAB-SIMULINK Subsystem Blocks

In this appendix the block diagrams represent the subsystems which are modeled by mathematical equations in chapter 3. With the help of these blocks the wind energy conversion systems which are described in chapter 4 are simulated.
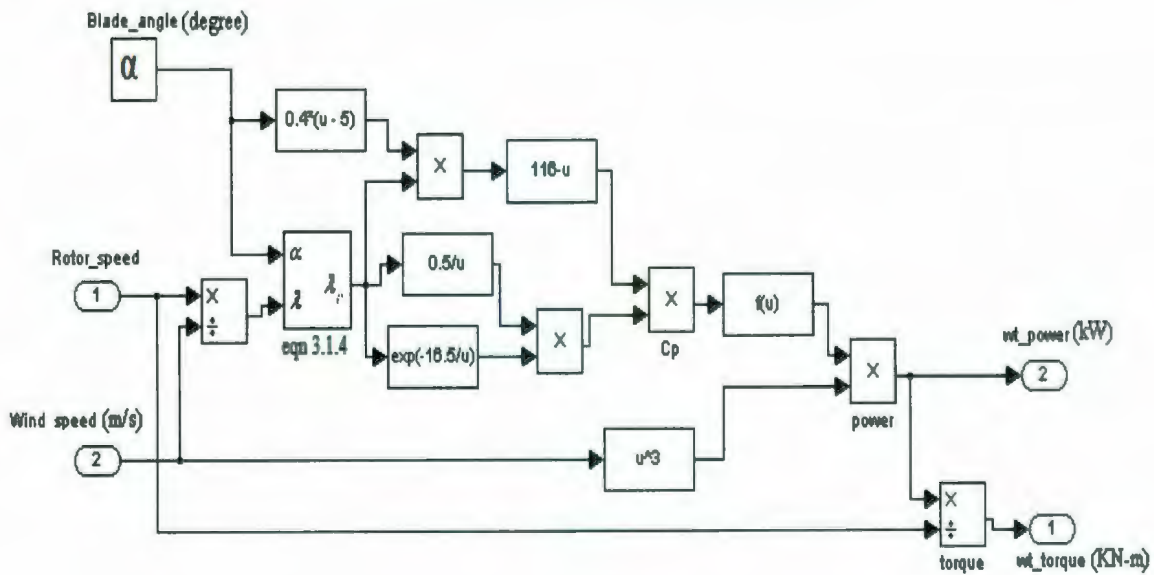

Figure A.1: Subsystem: 'SS Wind Turbine'

The Simulink block diagram of figure A.1 represents a WECS sub-system. This model is implemented in SIMULINK with the help of equations 3.1.1 to 3.1.4 in chapter 3. A fixed speed wind turbine is considered in chapter 3. Wind speed and rotor speed are

the variable input to this sub-system. Wind turbine torque and power are the output of this sub-system.
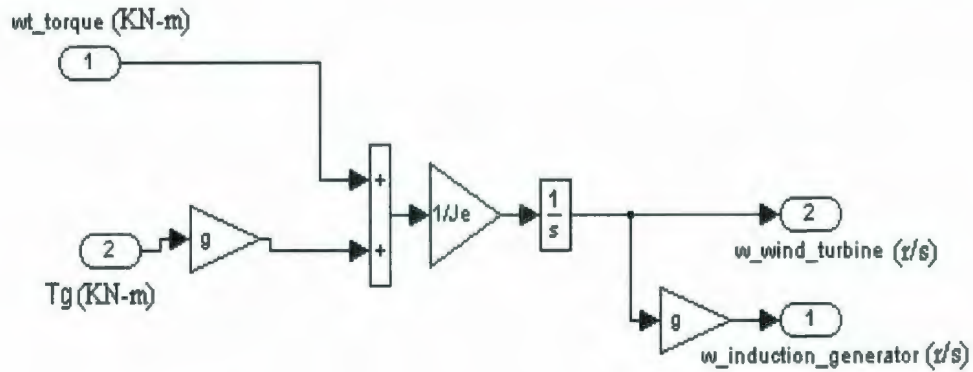
Figure A.2: Subsystem: 'SS Gear Box'

The block diagram of figure A.2 represents the gearbox sub-system in the wind turbine. This subsystem is implemented by equation 3.1.5 and 3.1.6. There are two inputs to this subsystem. One input is wind turbine torque and the other one is induction generator torque. There are again two outputs from this subsystem. One of them is turbine rotor speed and the other one is induction generator speed.
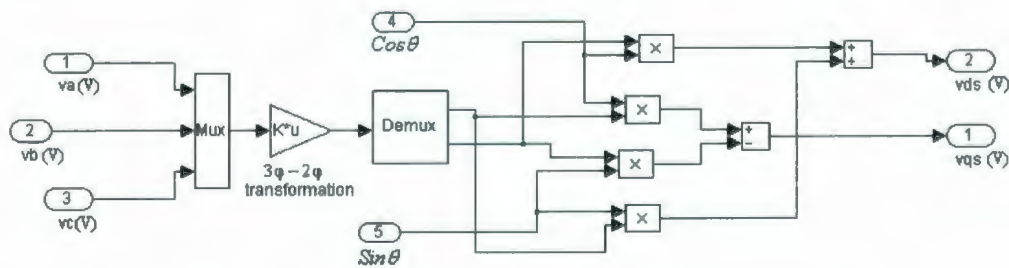

Figure A.3: Subsystem: 'SS abc-dq transformation'

The above SIMULINK block diagram of figure A.3 represents the subsystem for transforming three phase quantity to d-q axis quantity. The transformation was done

according to the Krause's method [27]. In this subsystem the three phase voltage and their angles are the input and d-q axis voltages are the outputs. This block was used in both the induction and synchronous machines.
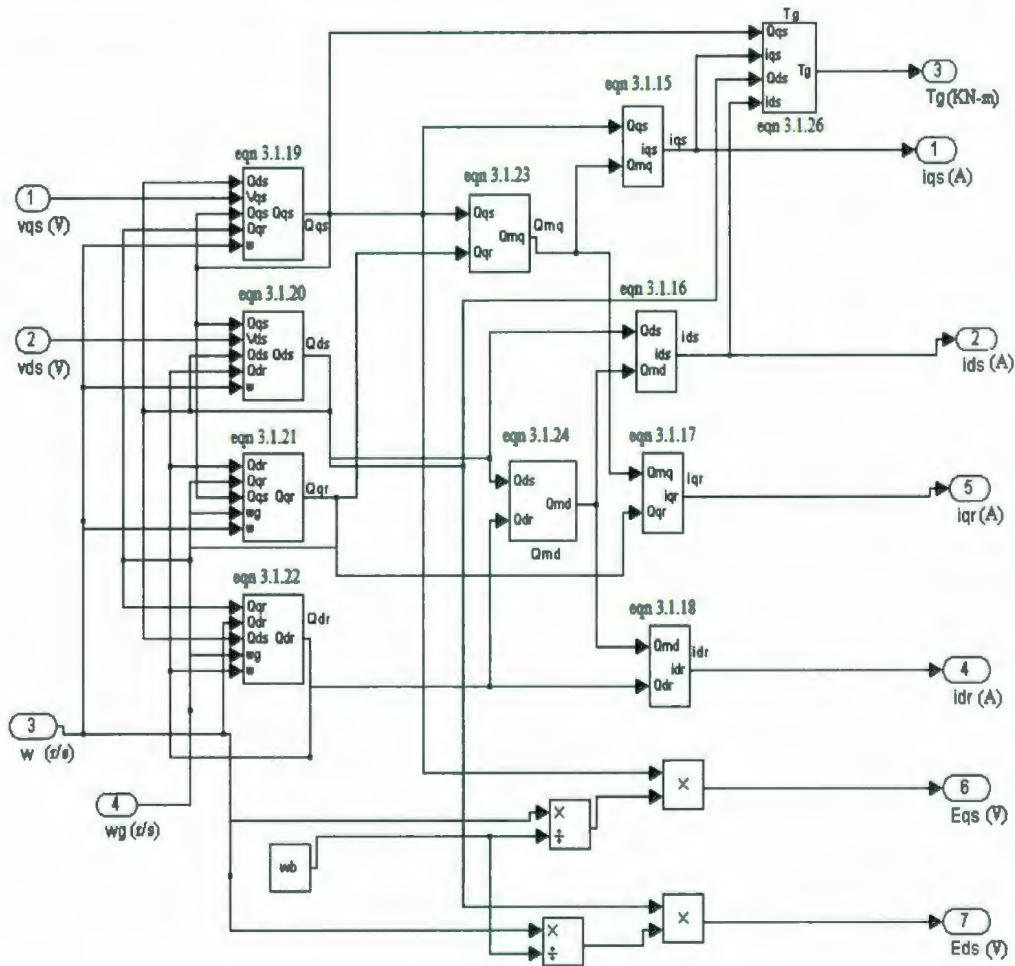

Figure A.4: Subsystem: 'SS Induction generator'

The subsystem of figure A.4 represents the Simulink representation of the induction machine's flux and current equations (3.1.15 to 3.1.24 and 3.1.26). The inputs to the subsystem are d-q axis voltage and rotor speed. The outputs from the subsystems are electromagnetic torque, d-q axis currents and voltages.

100
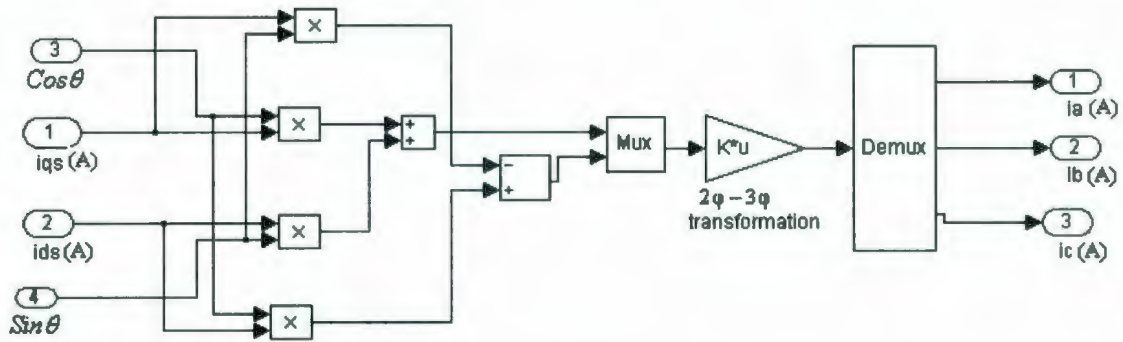
Figure A.5: Subsystem: 'SS dq-abc transformation'

The SIMULINK block diagram of figure A.5 is used for transforming d-q axis current quantity to three phase current. This SIMULINK block is simulated based on Krause's method [27]. This block is used in the induction and synchronous machines. In this subsystem d-q axis components and their angles are the input and the three phase currents are the output.
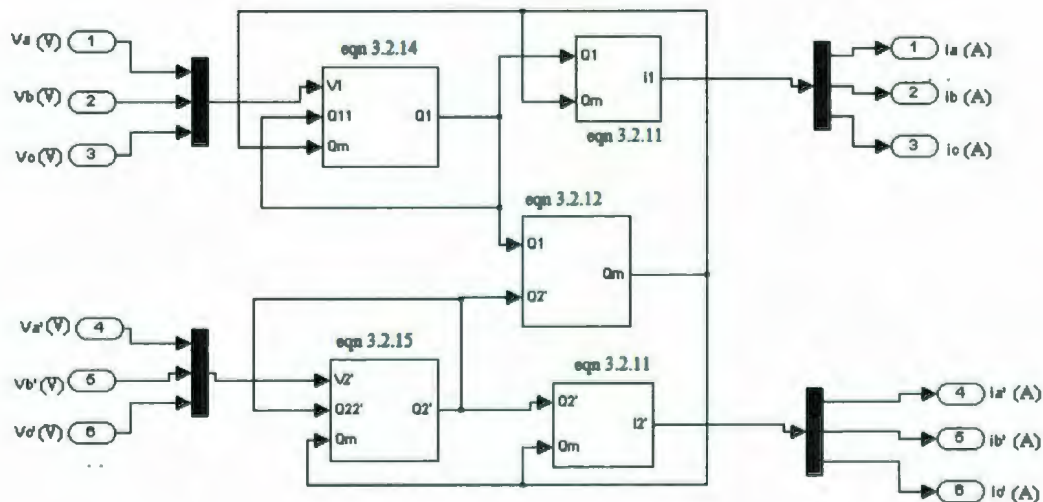
Figure A.6: Subsystem: 'SS Transformer flux and current'

The subsystem of figure A.6 represents the flux and current equations of a three phase transformer implemented by equations 3.2.11 to 3.2.15. In the above figure A.6

MUX and DE-MUX were used to reduce system complexity. In this case the three phase

voltages are the inputs and three phase currents are the outputs.

Figure A.7: Subsystem: 'SS Transmission line'

The above block diagram of figure A.7 represents a three phase transmission line.

Simulink blocks are used to implement equations 3.3.1 to 3.3.7. Here MUX and DE-

MUX were used to reduce the system complexity and also reducing the simulation time.

In this subsystem three phase currents are the inputs and three phase voltages are the

outputs in both sending end and receiving end. Depending on the length of transmission

line, signal delays are calculated in the time delay block.

Figure A.8: Subsystem: 'SS Synchronous generator flux and current'

The subsystem of figure A.8 represents the synchronous machine's flux and current equations from 3.4.7 to 3.4.23. In this subsystem d-q axis voltage, field voltage and rotor speed are the input to the subsystem. The electromagnetic torque and d-q and damping current components are the output from this subsystem.
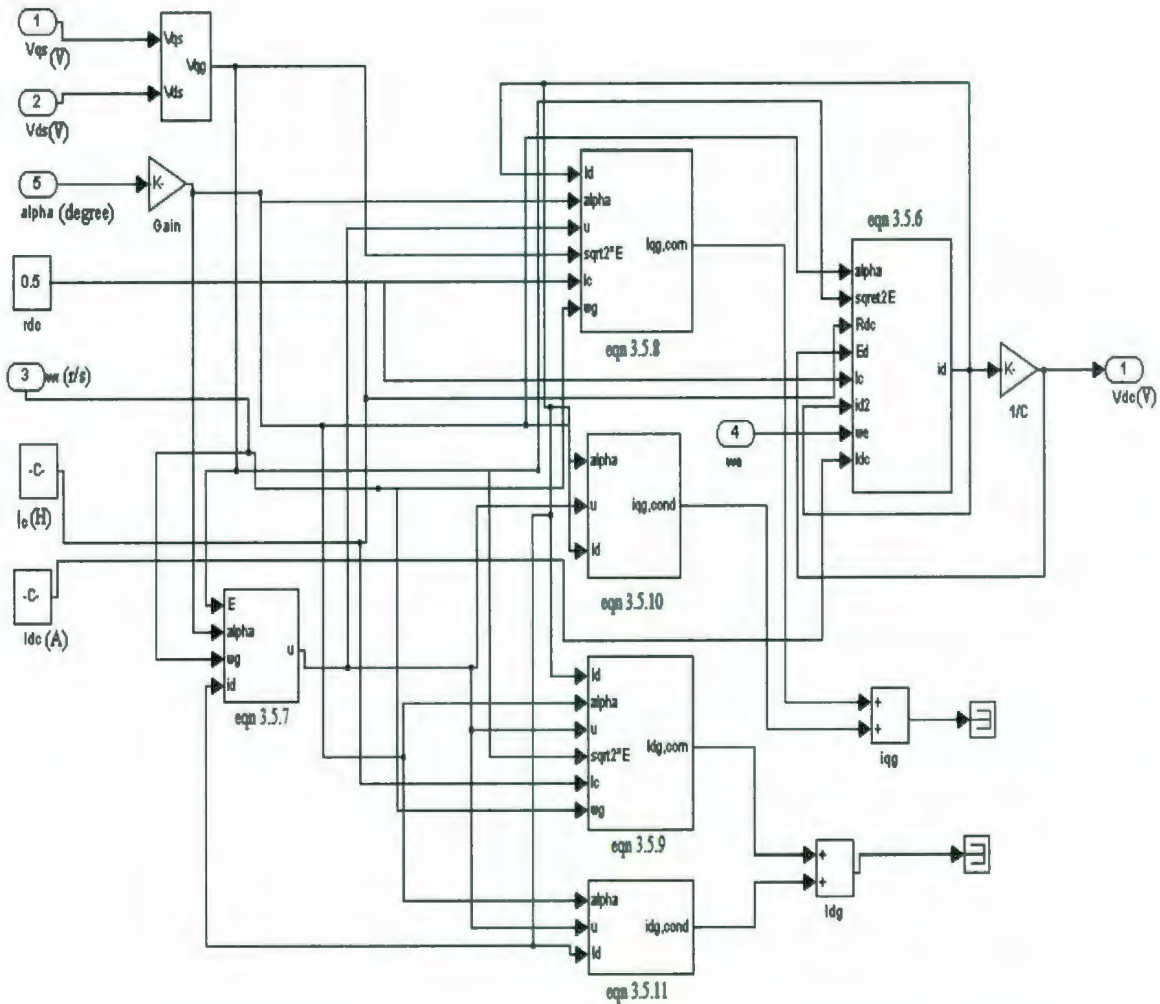
Figure A.9: Subsystem: 'SS Three phase current and voltage converter'

The block diagram of figure A.9 represents the converter which was simulated in Simulink with the help of equations 3.5.6 to 3.5.11. The output of this subsystem is the dc voltage which was fed to the synchronous machines dc field. The input to this subsystem is the d-q axis voltage and the firing angle. The gain block in the above subsystem is used to convert the unit of firing angle from degree to radian.

104

Appendix B

MATLAB Files

Wind-Diesel Model Parameters

fb=60;   % System frequency

wb=2*pi*fb;   % base speed

% initialization of Synchronous Machine

rs=0.234;   % Stator winding resistance

rf=0.005;   % Field winding resistance

rkd=0.00736;   % d-axis damper winding resistance

rkq1=0.008;   % q-axis damper winding-1 resistance

rkq2=0.005;   % q-axis damper winding-2 resistance

Xls=1.1458;   % stator winding leakage reactance

Xq=0.5911;   % q-axis winding reactance

Xd=0.0467;   % d-axis winding reactance

Xlf=0.0523;   % field winding leakage reactance

```
Xlkd=0.1970;                          % d-axis damper winding leakage reactance
Xlkq1=0.0578;                         % q-axis damper winding-1 leakage reactance
Xlkq2=0.7689;                         % q-axis damper winding-2 leakage reactance
p=2;                                  % no of synchronous machines pole
α=-0.83;                              % wind turbine blade angle
Jg=30.2;                              % Synchronous machine's rotor inertia constant
Jd=10.107;                            % diesel engines inertia constant
gd=1;                                 % diesel engine gear box ratio
Je=Jg+Jd/gr^2                         % equivalent inertia constant of diesel generator
```

% Synchronous machine's mutual reactance calculations

```
Xmq=1/(1/Xq+1/Xlkq1+1/Xlkq2+1/Xls); % q-axis magnetizing reactance
Xmd=1/(1/Xd+1/Xlkd+1/Xlf+1/Xls);      % d-axis magnetizing reactance
```

% Initialization of Wind Turbine parameters

```
Rr=1.083;                             %rotor winding resistance
Rs=1.015;                             %stator winding resistance
Lls=0.005974;                         %stator leakage inductance
Llr=0.005974;                         %rotor leakage inductance
Lm=0.2037;                            %magnetizing inductance
p=2;                                  %number of induction machine's poles
Jg=252.02;                            %Induction machine's moment of inertia
Xls=wb*Lls;                           % stator winding impedance
Xlr=wb*Llr;                           % rotor winding impedance
Xm=wb*Lm;                             %magnetizing impedance
Xmstar=1/(1/Xls+1/Xm+1/Xlr);          % total magnetizing impedance
Jt=98500;                             % turbine rotor moment of inertia
gr=50.5;                              % gear box ratio
Je=Jg+Jt/gr^2;                        % equivalent moment of inertia
Rt=21;                                % wind turbine radius
```

% Initialization of Transmission line parameters

d1 = 3.8;	% 3.8 kilometre long
d2=2.4;	% 2.4 kilometre long
d3=4.16;	% 4.16 kilometre long
d4=0.6;	% 0.6 kilometre long
d5=6.5;	% 6.5 kilometre long
R = 0.01123;	% resistance of line,Ohm per kilometre
L = 2.97e-3;	% inductance of line,Henry per kilometre
C = 0.174e-6;	% capacitance of line, Farad per kilometre
Zc = sqrt(L/C)	% characteristic impedance in ohms
tdelay1 = d1*sqrt(L*C)	% propagation delay in 3.8km line
atten1 = exp(-(R/2)*sqrt(C/L)*d1)	% attenuation in 3.8km line
tdelay2 = d2*sqrt(L*C)	% propagation delay in 2.4km line
atten2 = exp(-(R/2)*sqrt(C/L)*d2)	% attenuation in 2.4km line
tdelay3 = d3*sqrt(L*C)	% propagation delay in 4.16km line
atten3 = exp(-(R/2)*sqrt(C/L)*d3)	% attenuation in 4.16km line
tdelay4 = d4*sqrt(L*C)	% propagation delay in 0.6km line
atten4 = exp(-(R/2)*sqrt(C/L)*d4)	% attenuation in 0.6km line
tdelay5 = d5*sqrt(L*C)	% propagation delay in 6.5km line
atten5 = exp(-(R/2)*sqrt(C/L)*d5)	% attenuation in 6.5km line

% Initialization of Load parameters

Vrated =4.2e3	% 4.16KV system
SL = 200e3*(0.8 +j*0.6)	% 200 KW, 0.8 pf lagging
ZL = Vrated^2/conj(SL)	% phase load impedance in Ohms
RL = real(ZL)	% series RL load model resistance
LL = imag(ZL)/wb	% series RL load model inductance

% Initialization of transformer initialization

r1=0.025;	% primary winding resistance
xl1=0.056;	% primary winding leakage reactance

```
r2p=0.0134;                    % Secondary winding resistance refer to primary
xl2p=0.056;                    % Secondary winding leakage reactance refer to primary
xm1=708.8;                     % transformer magnetizing reactance
xm=1/(1/xl2p+1/xl1+1/xm1);     % transformer equivalent magnetizing reactance
NpbyNs=600/4200;               % transformer ratio (primary to secondary)
Ns/Np=1/NpbyNs;                % transformer ratio (secondary to primary)
```

Appendix C

Initial Site Assessment of Wind Farm near St. Anthony

An assessment of various sites around St. Anthony was done many years ago [34]. Initially ten sites were selected in that pre feasibility study. Long term wind statistics were only available for St. Anthony area in general; wind data for individual site was not available. The province of Newfoundland has a rugged topography. Hills, ridges and mountains cover the countryside. Large, flat open areas are rare in the province. It is extremely difficult to locate a site near roads and transmission lines that is easily accessible and that is higher than the surrounding area in a 10km radius. The point allocation was based on wind speed and direction distribution graphs for the region. In designing a wind farm, there is an obligation to ensure the protection of health, safety and welfare of others. Potential dangers include electrical shock, thrown ice, flying rotor blades and collapse of the structure. It is recommended that wind farm site be situated at least 750ft from the nearest housing.

Atmospheric ice accumulation on wind turbine blades, towers and transmission lines can affect the efficiency and continuous operation of installation and may cause structural damage. It appears icing is a potential hazard in St. Anthony area. A wind farm may have to be shut down for a short periods of time if excessive icing occurs. The geology of a site is a necessary consideration in site selection since it determines the ease by which the wind farm can be constructed. There are four basic types of surface conditions found in the province of Newfoundland: thinly covered bedrock, till, bog and forest. Smooth bedrock is ideal for a wind farm since preparation is limited and no major foundation is required. Site selection in forest area was avoided since higher towers are required in order to reduce sheltering effect and turbulence caused by the surrounding trees. All of the proposed areas were considered to have equal accessibility by sea, road and air. All of the initial sites would require construction or upgrading of access roads. The site requiring the most expensive construction did not receive any points. Points for other sites were awarded on the basis of their relative costs between the most expensive and least expensive access roads. Social impacts in all sites are expected to be similar. Acquisition of land is of prime importance in final selection of sites. If for some reason the site was privately owned and acquisition was either unfeasible or not possible, the site was disqualified. The visibility of wind farm is important in this study because the project may be the first of its kind in the province. A wind turbine is a potential source of electromagnetic interference, primarily in microwave and television interference. Here sites can only be selected if they are not in a direct line of transmission. The locations of all transmitting and receiving towers in the area were obtained from Canadian Coast Guard and the department of Communications. The connection distance is the length of

transmission line that is required to connect the wind farm to the existing distribution lines. This is an important factor from the point of view of economic feasibility. For the purpose of evaluation, we assumed that the line will follow the access road and thus site conditions are not critical in transmission line construction. Based on above criteria a decision matrix [34] was developed to assist in making an initial investigation and deciding as to the wind potential region and a particular site within that region. This methodology was designed on the basis of an evaluation matrix which permits the assigning of numerical values to relevant characteristics of potential wind farm sites such that the site may be compared and the best site chosen. The weighing values given each category are based on that category's importance in regard to the applicability of a site to support a wind farm. Based on decision matrix all sites were ranked in Table C.1 is given below.

Table C.1: Ranking of Initial wind farm sites near St. Anthony

Ranking	Community	Site No.	Score
1	Cape Norman	10	155
2	Cook's Harbour	9	150
3	St. Anthony	3a	145
4	L' Anse aux Meadows	7	130
5	Ship cove	8	115
6	St. Carrol's	4	110
7	White cape	5	110
8	Goose cove#2	2	105
9	Cape raven	6	105
10	Goose cove#1	1	100

Maximum available point 160